



Neurotoxicity and endocrine disruption caused by polystyrene nanoparticles in zebrafish embryo



Mónica Torres-Ruiz^a, Mercedes de Alba González^a, Mónica Morales^b, Raquel Martín-Folgar^b, M^a. Carmen González^a, Ana I. Cañas-Portilla^{a,*}, Antonio De la Vieja^{c,**}

^a Environmental Toxicology Unit, Centro Nacional de Sanidad Ambiental (CNSA), Instituto de Salud Carlos III (ISCIII), Ctra. Majadahonda-Pozuelo Km. 2,2., Majadahonda, Madrid 28220, Spain

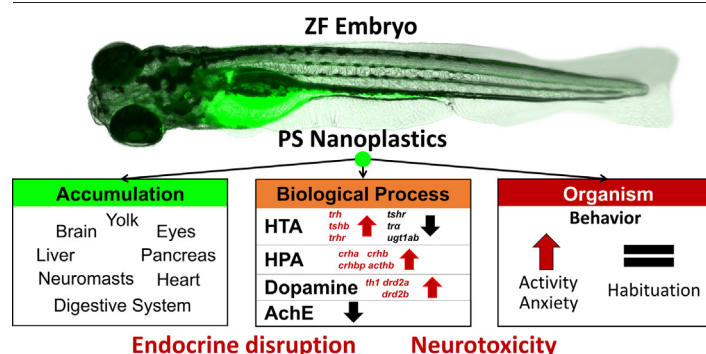
^b Grupo de Biología y Toxicología Ambiental, Departamento de Física Matemática y de Fluidos, Facultad de Ciencias, UNED, Urbanización Monte Rozas, Avda. Esparta s/n, Ctra. de Las Rozas al Escorial Km 5, 28232 Las Rozas, Madrid, Spain

^c Endocrine Tumor Unit, Unidad Funcional de Investigación en Enfermedades Crónicas (UFIEC), Instituto de Salud Carlos III (ISCIII), Ctra. Majadahonda-Pozuelo Km. 2,2., Majadahonda, Madrid 28220, Spain

HIGHLIGHTS

- Polystyrene NP neurotoxicity and endocrine disruption studied in zebrafish embryos.
- NP accumulated in brain and sensory organs.
- NP altered behavior: effects on activity and anxiety but not learning.
- NP altered neuroendocrine gene expression and neurotransmitter metabolism (AChE).
- NP adverse outcome pathway for neurotoxicity and endocrine disruption is proposed.

GRAPHICAL ABSTRACT



ARTICLE INFO

Editor: Henner Hollert

Keywords:
Nanomaterial
Plastic
Development
Toxicity
Behavior
Hormones

ABSTRACT

Nanoplastics (NP) are present in aquatic and terrestrial ecosystems. Humans can be exposed to them through contaminated water, food, air, or personal care products. Mechanisms of NP toxicity are largely unknown and the Zebrafish embryo poses an ideal model to investigate them due to its high homology with humans. Our objective in the present study was to combine a battery of behavioral assays with the study of endocrine related gene expression, to further explore potential NP neurotoxic effects on animal behavior. Polystyrene nanoplastics (PSNP) were used to evaluate NP toxicity. Our neurobehavioral profiles include a tail coiling assay, a light/dark activity assay, two thigmotaxis anxiety assays (auditory and visual stimuli), and a startle response - habituation assay in response to auditory stimuli. Results show PSNP accumulated in eyes, neuromasts, brain, and digestive system organs. PSNP inhibited acetylcholinesterase and altered endocrine-related gene expression profiles both in the thyroid and glucocorticoid axes. At the whole organism level, we observed altered behaviors such as increased activity and anxiety at lower doses and lethargy at a higher dose, which could be due to a variety of complex mechanisms ranging from sensory organ and central nervous system effects to others such as hormonal imbalances. In addition, we present a hypothetical adverse outcome pathway related to these effects. In conclusion, this study provides new understanding into NP toxic effects on zebrafish embryo, emphasizing a critical role of endocrine disruption in observed neurotoxic behavioral effects, and improving our understanding of their potential health risks to human populations.

* Correspondence to: A.I. Cañas-Portilla, Centro Nacional de Sanidad Ambiental (CNSA), Instituto de Salud Carlos III (ISCIII), Ctra. Majadahonda-Pozuelo Km. 2,2., Majadahonda, Madrid 28220, Spain.

** Correspondence to: A. De la Vieja, Endocrine Tumor Unit, Unidad Funcional de Investigación en Enfermedades Crónicas (UFIEC), Instituto de Salud Carlos III (ISCIII), Ctra. Majadahonda-Pozuelo Km. 2,2., Majadahonda, Madrid 28220, Spain.

E-mail addresses: mtorres@isciii.es (M. Torres-Ruiz), acanas@isciii.es (A.I. Cañas-Portilla), adelavieja@isciii.es (A. De la Vieja).

<http://dx.doi.org/10.1016/j.scitotenv.2023.162406>

Received 4 December 2022; Received in revised form 5 February 2023; Accepted 18 February 2023

Available online 23 February 2023

0048-9697/© 2023 The Authors. Published by Elsevier B.V. This is an open access article under the CC BY license (<http://creativecommons.org/licenses/by/4.0/>).

1. Introduction

Plastic production has increased exponentially and by 2018, total human plastic waste amounted to 6900 million tons (Letcher, 2020). Plastic reaches aquatic, terrestrial and atmospheric environments (Rhodes, 2018; Zhang et al., 2020b) and suffers physical and chemical degradation resulting in microplastic (MP) (< 5 mm) and nanoplastic (NP) (< 0.001 mm) generation (Andrady, 2017; Gigault et al., 2018). Humans are exposed to NP mainly by consuming contaminated food (marine and terrestrial organisms) and drinking water, but also by inhalation and dermal contact (Chang et al., 2020). Even though detection of NP in human matrices has not been technically possible so far, MP have been found in human blood, lung tissue, gastrointestinal tract, and placenta (Gruber et al., 2022; Jenner et al., 2022; Leslie et al., 2022; Ragusa et al., 2021; Schwabl et al., 2019). Nevertheless, in vitro and in vivo experiments have demonstrated that NP have the potential to penetrate different biological barriers including gastrointestinal and brain blood barriers, and have been detected in many important organs such as brains, the circulation system, and livers of model animals (Deville et al., 2015; Hwang et al., 2022; Peng et al., 2020; Walczak et al., 2015).

In recent years, the potential toxic effects of nanoplastics have been studied in a variety of aquatic and terrestrial organisms, and these have been shown to range from metabolism disruption to developmental, fertility, and behavioral problems (Chae and An, 2020; Chae and An, 2017; Li et al., 2022; Liu et al., 2021b; Liu et al., 2019; Matthews et al., 2021; Ullah et al., 2023). In vitro effects in human tissue cultures have also been reported, such as oxidative stress, and inflammation in lung, skin, and gastrointestinal cells (Lehner et al., 2019). Neurodevelopmental effects of NP have been shown in rodents, with molecular and functional alterations in the central nervous system (CNS) and cognitive deficits (Jeong et al., 2022). However, other studies have found no behavioral alterations in mice exposed to small size (~ 20 nm) NP (Estrela et al., 2021).

The zebrafish (ZF) embryo (*Danio rerio*) has been recommended as an inexpensive, quick, and easy model to assess NP toxicity (Torres-Ruiz et al., 2021). This fish is a small cyprinid with many advantages for toxicological research such as transparency of the embryo, a completely sequenced genome, high egg production and no major rearing difficulties (Bourdineaud et al., 2013). Moreover, it shares a high genetic sequence homology with humans, with 71.4 % of total genes and 84 % of human-disease genes having a human orthologue (Howe et al., 2013). ZF have become an excellent vertebrate model for neurotoxicity research because they retain neurological systems very similar to those of mammals (d'Amora and Giordani, 2018). Therefore, this fish is the perfect model to study both environmental and human health effects of NP.

Indeed, in the last few years, there has been an increase in studies evaluating effects of NP on the ZF embryo development (Bhagat et al., 2020). For the most part, results show NP accumulate in several ZF organs and can cause behavioral neurotoxic effects, together with general downregulation of central nervous system and sensory genes (Torres-Ruiz et al., 2021). NP have been observed to alter larvae locomotion, although degree and direction of effects are still unclear (Brun et al., 2019; Chen et al., 2017; Liu et al., 2022; Manuel et al., 2022; Pedersen et al., 2020; Pitt et al., 2018; Teng et al., 2022). Most studies have used the light/dark locomotion assay and both hyperactivity, hypoactivity, and no alterations have been reported, regardless of NP size or concentration (Torres-Ruiz et al., 2021). However, we have found no study evaluating other important potential effects on behaviors such as anxiety or habituation. In addition, little is known so far about the effect of NP on embryo tail coiling, a behavior indicating early motor activity generated by muscle innervation (Kimmel et al., 1974).

Different mechanisms of NP toxicity have been proposed and include oxidative stress (Chen et al., 2017), immune responses (Brun et al., 2018), and alterations in energy metabolism (Trevisan et al., 2019). However, other processes could play a role, considering the variety of behavioral responses observed (Torres-Ruiz et al., 2021). Of special interest is the role of NP as potential endocrine disruptors. Although very few data exist on the

matter, some authors have shown NP can affect thyroid-regulating hormones (Amereh et al., 2019; Zhao et al., 2020). Since it is well known that endocrine disruption can affect CNS development (Serolini and Jungers, 2021) and cause behavioral alterations (Repouskou et al., 2020; Tao et al., 2022), this is an essential toxicity pathway to explore.

There is clearly a need to advance in the knowledge of NP potential toxicity mechanisms, including endocrine-related neurotoxicity, and how this could translate into changes in development and behavior. Therefore, our objective in the present study was to combine a battery of behavioral assays with the study of endocrine related gene expression, to further explore potential NP effects on animal behavior. Our neurobehavioral profiles include the tail coiling assay, the light/dark activity assay, two thigmotaxis anxiety assays (auditory and visual stimuli), and a startle response - habituation assay in response to auditory stimuli. To the best of our knowledge, our study is the first to combine these assays to evaluate behavioral alterations in response to NP exposure and potential role of endocrine disruption.

2. Materials and methods

2.1. Nanoplastics concentrations

Polystyrene nanoplastics (PSNP) were used as representatives of plastic particles due to their commercial availability in a well characterized specific size and shape, and the possibility of purchasing fluorescently labelled particles. In addition, polystyrene is one of the main plastic types used for many commonly used items such as insulating styrofoam, toys, food containers, etc., and its degradation into nanoparticles has been observed under laboratory conditions (Kik et al., 2020). Fluorescently labelled (Firefli™ Fluorescent Green) and pristine polystyrene particles with a mean diameter of 30 nm were purchased from Fisher Scientific (Madrid, Spain), catalogue number Thermo Scientific™ G25 and 5003A respectively. PSNP of 1.05 g/cm³ density were provided as a 1 % and 10 % solution in water respectively, both with <2 % anionic surfactant (proprietary, similar to SDS) to prevent agglomeration, and <0.05 % the antibacterial agent NaN₃ (only fluorescently labelled particles). Stock solutions were prepared to working concentrations in embryo medium and thus the additives were diluted enough not to cause effects in embryos (Wang et al., 2015; Pedersen et al., 2020). As per manufacturer instructions, stock solutions were shaken and sonicated for 1 min prior to use. In addition, every time ZF medium was changed, solutions were shaken and sonicated for 3–5 min prior to use.

PSNP working concentrations were chosen carefully, after a pilot study, to better appreciate effects (unpublished work), and reflect possible environmentally relevant concentrations (up to 9 mg/L; see Gallego-Urrea et al., 2010, Torres-Ruiz et al., 2021, and Materić et al., 2022c). In this prior study, embryos were exposed to solutions of 0.2, 1, and 5 mg/L of fluorescently labelled particles (for 120 h) to observe mortality, skeletal abnormalities (lordosis), and location of PSNP accumulation in the embryos. Since 60 % mortality was observed at 5 mg/L, concentrations for sub-lethal toxicity evaluations with pristine particles were chosen to be 0.1, 0.5, and 3 mg/L.

2.2. Nanoplastics characterization

PSNP solutions in embryo water at the concentrations used for exposure were characterized by observation under a transmission electron microscope (TEM) FEC Tecnai 12 operated at 120 kV. Briefly, samples were sonicated for 3–5 min, then incubated on copper grids for 10 min, washed with MQH₂O and then dyed with 2 % uranyl acetate before observation. To assess particle size distribution in embryo medium, PSNP solutions were characterized using nanoparticle tracking analysis (NTA). For this we have used the NanoSight NS3000 (Malvern Instruments GmbH, United Kingdom) equipped with a high sensitivity sCMOS camera. Three replicates for each PSNP assay concentration (0.1, 0.5, and 3 mg/L) were introduced automatically and videos of 30 s were recorded at 30 frames per second. Software NTA 3.0 was used to monitor individual particles. In addition, particle z

potential in the same solutions was determined with the Zetasizer Nano SZ (Malvern Instruments GmbH, United Kingdom).

2.3. Zebrafish husbandry

Adult wild type zebrafish (*Danio rerio*) from Instituto de Salud Carlos III (Majadahonda-Madrid, Spain) animal facility were maintained in glass recirculating aquariums at 25–26 °C, pH between 7 and 7.5, oxygen levels 6–6.5 mg/L, and conductivity 500–600 µS/cm. Water for fish was prepared using deionized water from a MilliQ system (Merck RiOs™ Essential 24) and a mixture of salts: Cl₂Ca.2H₂O (294 mg/L), MgSO₄.7H₂O (123 mg/L), NaHCO₃ (64.7 mg/L), and KCl (5.8 mg/L). Fish tanks were gently cleaned and water was renewed three times a week to ensure suitable NH₄, NO₂, and NO₃ levels (< 0.05 mg/L for the first two; < 5 mg/L for nitrate). Nitrogen compounds, oxygen, conductivity, and pH were measured once a week. Fish were maintained in a light/dark cycle of 14:10 h and they were fed twice a day with frozen brine shrimp (*Artemia salina*, Ocean Nutrition™, Belgium), shell free brine shrimp eggs (Ocean Nutrition™, Belgium) or Tropicana Basic fish flakes (Dajana®, Czech Republic). Our fish laboratory adheres to directive 2010/63/EU on the welfare of animals.

2.4. Embryo culture and Nanoplastic exposure

Embryos were obtained by placing a breeding tank inside the aquarium. Fish bred after the onset of light (at 8 am) and embryos were collected within 1 h of oviposition. Embryos were washed with embryo water (same as fish water, see above) and placed in large Petri dishes. Eggs were observed under a stereoscope (Olympus) and fertilized eggs were placed in 24 well plates for PSNP exposure within 2 h of oviposition. PSNP solutions were renovated every 24 h and the exposure lasted until 120 hpf. For fluorescently labelled particles (pilot study), one plate per PSNP concentration and one for negative control (embryo water) were used, with 2 mL solution per well. In the main study using pristine particles, three plates (24 wells) per PSNP concentration and negative controls (embryo water) were used for a total of 72 embryos per treatment/control. Specific number of embryos for endpoint is as follows: mortality and hatching 72; tail-coiling 48; biometry: 24; locomotion: 48.

Plates were kept in an incubator (Nuair) at 28 °C until the end of the study (120 hpf) and medium was renewed every 24 h. Mortality was assessed every 24 h and dead embryos were removed.

2.5. Nanoplastic bioaccumulation observation

Zebrafish larvae (treated with 0.1 and 0.5 mg/L) were observed for fluorescent PSNP accumulation in different organs at 24, 48, and 72 hpf, after being rinsed with embryo water to avoid background fluorescence. Larvae were photographed using a Stellaris 8 confocal fluorescent microscope (Leica Microsystems) using objective HC PL APO 20 × / 0.75 CS2. In all experiments, digitalized images were captured using Leica LasX v. 4.5 software.

2.6. Zebrafish behavioral analysis

Tail bursting of embryos (non-dechorionated) was assessed at 24 ± 2 hpf, a time when tail coiling is constant (De Oliveira et al. 2021). Embryos of each treatment were transferred to a large petri dish (100 mm) with embryo water and 2 × 1 min videos (5 frames per second - fps) were recorded (AxioCam 208 coupled with Discovery V12 stereoscope, Carl Zeiss, Germany) at constant room light and temperature, and without embryo disturbance. To minimize time out of the incubator, videos were done in groups of 24 embryos at a time. Later these videos were analyzed using the Danioscope software (Noldus Information Technology, Netherlands) and tail activity was assessed by the following parameters: % burst activity (percent time embryo's tail is moving), mean burst duration (mean of all tail

coiling durations), and burst count per minute (number of tail coils per minute).

At 120 hpf larvae were assessed for **swimming activity** in a light/dark locomotor response test using a DanioVision Observation Chamber (Noldus Information Technology, Netherlands), using the DanioVision Temperature Control Unit (Noldus Information Technology, Netherlands) to ensure a constant temperature at 28 °C. Larvae (in 24-well plates) were conditioned in the dark for 10 min, followed by 3 cycles of light stimulus (5 min under white light/5 min in the dark), and ending with 5 min in the dark. Videos were taken at 25 fps using an infrared sensitive camera and analyzed using the software Ethovision XT® (v.15, Noldus Information Technology, The Netherlands) for total distance moved (mm) and velocity (mm/s) in each condition (light or dark periods).

In addition, a **vibration startle response** (tapping) and **habituation** experiment was performed at 120 hpf using the DanioVision Observation Chamber coupled with a tapping device, in the dark and at a constant temperature of 28 °C. Larvae were conditioned for 5 min and a first cycle of 30 taps, with 1 tap per second, at the loudest noise level (intensity = 8), was followed by 15 min of quiet time. Immediately after, larvae were subjected to a second tapping interval, with the same regime as the first one (30 taps, 1/s) and the experiment ended with a 1-min quiet time (Faria et al., 2019). Caution was taken to prevent any loud ambient noises from occurring during this experiment. Later, videos (25 fps) recorded were analyzed using the Ethovision XT 15 software for distance moved by larvae during 1 min prior to tapping, during the first tapping episode (30 s), during 1 min before the second tapping interval, and during the second tapping interval (30 s). Distance moved was calculated in 1-s intervals. To compare habituation velocity between treatments, we calculated the slope of the line that resulted from plotting distance traveled vs. time during both tapping periods.

Larvae anxiety-like behavior in response to visual (light) and auditory (tapping) stimuli was studied by investigating thigmotaxis (wall-hugging) behavior. For this, videos recorded for the light/dark or tapping experiments were re-analyzed using a different arena settings option in Ethovision software. Each arena (each well area) was separated into two zones, the “center”, comprised of a circle of 10 mm in diameter drawn in the center, and the “edge”, comprised of the area between the inner circle and the well borders (4 mm width). The use of a 24-well plate allows for both zones to cover equivalent spatial areas and thus prevent the bias of zone size differences (Schnörr et al., 2012). Thigmotaxis was assessed by evaluating percent time spent by larvae in the center vs. the edge of the wells using light/dark or tapping stimuli.

2.7. Zebrafish biometry

Larvae length (front part of the head to end of last somite), and areas representing head, eye, pericardium, and yolk sizes were measured in each larvae/treatment at 72 hpf. Each larva was photographed at 20 × magnification using a Zeiss stereoscope and an AxioCam 208 camera (Carl Zeiss, Germany). Larvae were anesthetized with MS-222 (tricaine methanesulfonate) 0.1 mg/mL before photographing. The Danioscope software (Noldus, The Netherlands) was used to calculate lengths and areas in pixels that were converted to mm using a calibration ruler photographed at the same magnification as larvae. Larvae used for biometry were later discarded and not used in locomotion experiments.

2.8. RNA isolation and quantitative real-time polymerase chain reaction (qRT-PCR)

Total RNA extraction from 30 larvae ($n = 3$ replicates) was performed using easy-RED™ Total RNA Extraction Kit (iNtRON-Biotechnology) following manufacturer instruction. Reverse transcription (RT-PCR) was performed using M-MuLV Reverse Transcriptase (New England Biolabs Inc.) to obtain cDNA, and amplified by polymerase chain reaction (PCR) using LinusTaq Master Mix Ready to Load with 7.5 mM MgCl₂ (cmb) kit in a thermocycler (Biometra). The amplified product was separated in 1 %

agarose gel and identified using GelRed® Nucleic Acid Gel Stain (Biotium) in a UV system (Analytik Jena, Fisher scientific). Quantitative real-time PCR was done on a LightCycler 480II (Roche) using SYBR Green PCR kit (Takara Biochemicals). qRT-PCR reactions were conducted with the following parameters: initiated at 95 °C for 30 s, and 40 cycles of 5 s at 95 °C, 30 s at 60 °C, and 10 s at 72 °C. All samples were repeated in triplicates. Primers for the target genes and the reference gene applied in this study were designed or prepared according to other references (Table 1). Each expression of target genes was normalized to the housekeeping gene ribosomal protein L8 (*rpl8*) and then normalized to the control. A dissociation curve and a negative control of qRT-PCR without template were also conducted to ensure the specificity of the primer pairs and that the cDNA was not contaminated. The changes in the relative mRNA expression of target genes were quantified with 2-ΔΔCT method.

2.9. Acetylcholinesterase assay

The acetylcholinesterase (AChE) assay was done according to Küster (2005) with few modifications. Briefly, at 120 hpf, three replicates of 7 embryos each per PSNP concentration (0.1, 0.5, and 3 mg/L) were placed on ice in Eppendorf tubes, washed twice with MQH₂O and twice with cold homogenization phosphate buffer (0.1 M NaH₂PO₄·7H₂O with 0.1 % v/v Triton-X; pH 7.5). Larvae were then resuspended in 0.5 mL phosphate buffer and homogenized using glass tissue grinders. Homogenate was then centrifuged at 4 °C for 15 min at 12500 rpm and larvae supernatant was transferred to two Eppendorf tubes that were then frozen at -80 °C until analysis.

Colorimetric determination of AChE was done in triplicate for each sample replicate and AChE assay controls (phosphate buffer) in 96-well plates. Each well was filled first with 100 μL 5,5'-Dithiobis-(2-Nitrobenzoic Acid) (DTNB) 0.4 mg/mL, 80 μL phosphate buffer (0.1 M NaH₂PO₄·7H₂O, pH 7.5), and 20 μL larvae supernatant. After 10 min incubation at room temperature (24 °C) to correct non-specific spontaneous hydrolysis of DTNB, the reaction was started with the addition of 100 μL acetylthiocholine iodide (1.35 mM). Kinetic measurements of mean slope optical density per minute were registered at 412 nm for 10 min using a Spark® spectrophotometer (TECAN, Austria) and the software Sparkcontrol v2.2.

Enzyme activity was corrected for protein content. Concentration of protein was determined using the commercial kit QuantiPro™ BCA Assay (Merck, Spain) at 562 nm in triplicate for each sample replicate and blanks (phosphate buffer) using 25 μL of diluted embryo supernatant (1:20 in phosphate buffer). AChE activity inhibition was expressed as the percent of activity levels of exposed animals to the activity in controls.

2.10. Statistical analysis

All data were checked for normality and homoscedasticity using the Kolmogorov-Smirnov and Levene tests prior to analyses using the online free softwares <https://www.socscistatistics.com/tests/kolmogorov/default.aspx> and https://www.statskingdom.com/230var_levenes.html. Significant differences between control and each PSNP treatment were assessed by a two-tailed Student's *t*-test, using an a priori probability of a type I error of ≤0.05. Data are presented as means ± SE.

Table 1
Oligonucleotides sequences used for gene expression analysis.

	Gene		Name	Accession n°	Primer (5'-3')	bp	Reference	
Endocrine System	<i>trh</i>	Hypothalamus-pituitary-thyroid axis Endocrine-thyroid disruption	Thyrotropin releasing hormone	NM_001012365.2	F: GCTCTCTCCGTCGGTCTGT R: GCGAGATCCGTGCTGATGA	57	Chu S. et al. (2020)	
	<i>trhr</i>		Trh receptor	NM_001114688.1	F: CAGTGCCATCAACCCTCTGA R: GGCAGCGCGGAACCTTCT	55	Chu S. et al. (2020)	
	<i>tshb</i>		Thyroid stimulating hormone beta subunit	XM_021476792.1	F1: TAATGAAGGTTGCCGTGCT R1: AAACGAGGACCCACCAACTC	157	This study	
					F2: AATCCAGACCCTCCAGACAGA R2: CATAGGCACGGCAACCTTCA	105		
					F3: CACCTACCCAGTGGCACTTA R3: TCTCCTCGGGGTACAGATGA	128		
	<i>tshr</i>		Tsh receptor	NM_001145763.2	F: GCGCCAACCCTTTTCTGTAT R: CTCGTTTGCTCCTGTTTCT	182	Chu S. et al. (2020)	
	<i>tra</i>		Thyroid receptor alpha	NM_131396.1	F: AAGTGGATATAATCCGAACATAGGC R: ACGCCAATGCCACTTCCT	196	Chu S. et al. (2020)	
	<i>ugt1ab</i>		Glucuronosyl transferase	NM_213422.2	F: CCACCAAGTCTTTCCGTGTT R: GCAGTCCTCACAGGCTTTC	168	Zhai W et al (2014)	
	<i>crha</i>		Hypothalamus-pituitary-interrenal axis Endocrine-anxiety disruption	Corticotropin releasing hormone a	XM_009298729.3	F: ATTTAGTCGAACCGCAGCCA R: ATCTCAGTCGGTGTCTCCA	155	Chu S. et al. (2020)
	<i>crhb</i>			Corticotropin releasing hormone b	NM_001007379.1	F: TTCGGGAAGTAACCACAAGC R: CTGCACTTATTCGCTTCC	161	Tu X. et al (2020)
<i>acthb</i>	Adrenocorticotrophic hormone	NM_001083051.1		F: TATCGCATGACCCACTTCCG R: GGGGTTTGTGGATTCTGT	91	Tu X. et al (2020)		
<i>crhbp</i>	crh binding protein	NM_001003459.1		F: TCATCGGCGAACCTACTGAC R: CCTTCATCACCCAGCCATCA	105	Tu X. et al (2020)		
Central nervous system	<i>th1</i>	CNS system	Tyrosine hydroxylase	NM_131149.1	F: AGCGAGCAGATCGTGTGTTGA R: CCTCCAAGCCATCCTTTGGT	178	Tu X. et al (2020)	
	<i>drd2a</i>		Dopamine receptor D2a	NM_183068.1	F: TGCTCTCTGTGTGATTGCGA R: GCATGTGCGTTTGGTGTGGA	151	Tu X. et al (2020)	
	<i>drd2b</i>		Dopamine receptor D2b	XM_021476029.1	F: TGTGGGGATGGAAATGGTGG R: TGGACTGATATTCGGCGTGG	134	Tu X. et al (2020)	
	<i>rpl8</i>	HK gene	Ribosomal protein 8	NM_200713.1	F: TTGTTGTTGTTGTGCTGGT R: GGATGCTCAACAGGGTTCAT	136	Chu S. et al. (2020)	

3. Results

3.1. Nanoplastic characterization

Nanoplastics were characterized by TEM and individual particle size was confirmed to be 25 ± 0.6 nm in size. However, even though solutions were sonicated prior to analysis, aggregation of PSNP was observed at all tested concentrations (Fig. 1a). Particle aggregation was also evaluated by NTA. Aggregates had a mean particle size of 105.1 ± 27.4 nm (0.1 mg/L), 111.1 ± 40.8 nm (0.5 mg/L), and 134.4 ± 47.2 nm (3 mg/L) (Fig. A.1). Particle z potential had a mean of -13.6 ± 0.06 (0.1 mg/L), -16.1 ± 1.76 (0.5 mg/L), and -17.3 ± 0.21 (3 mg/L) (Fig. A.1).

3.2. PSNP accumulation

Nanoplastics accumulation was studied through the observation of fluorescent PSNP in ZF embryo. Pictures taken at 24 and 48 hpf show larvae start to accumulate PSNP inside the chorion but mostly in the yolk (Fig. 1 b, c). Pictures taken at 72 hpf show uptake in specific tissues that was dose dependent, with larvae exposed to 0.5 mg/L and higher (not shown) exhibiting overall background fluorescence suggesting whole body distribution (Fig. 1d). However, certain organs accumulated PSNP preferentially. The organ with the most fluorescence (PSNP accumulation) was the yolk, followed by the digestive tract, in particular the intestine, pancreas, and liver (Fig. 1e, h). The eyes showed substantial PSNP uptake (Fig. 1f) and other important organs such as the brain and neuromasts of the lateral line also showed PSNP buildup (Fig. 1f, g). No preferential PSNP accumulation was observed in the heart (Fig. 1h) and no PSNP fluorescence was observed in bone tissue (Fig. A.2).

3.3. Morphological abnormalities and mortality

Exposure to fluorescent PSNP for the preliminary study had an effect on mortality (60 %) and a 30 % lordosis rate only at the highest concentration (5 mg/L, data not shown). In the main study, no mortality was observed in animals exposed to pristine particles (highest concentration of 3 mg/L), but some morphological abnormalities were confirmed. Eye size was decreased significantly (6–11 %) in all treatments with respect to control with larvae treated at 3 mg/L having smaller eyes than larvae in the 0.1 and 0.5 mg/L treatments (Fig. 2a). Head size was decreased in a similar manner at all concentrations (~5 %; Fig. 2b), and pericardial area was significantly increased only at the highest concentration by 9 % (Fig. 2c). No effect was observed for yolk size (Fig. 2d), otolith diameter (Fig. 2e), or body length (Fig. 2f).

3.4. Effects on activity/behavior

Animals exposed to PSNP showed significant alterations in activity patterns (Fig. 3). At 24 hpf, tail activity (bursts/min) increased significantly in a concentration dependent manner with increases of 33, 51, and 55 % for larvae exposed to 0.1, 0.5, and 3 mg/L respectively (Fig. 3a). Interestingly, despite increase number of bursts per minute, mean burst duration, which denotes burst quality, decreased in all treatments, being significant for 0.5 mg/L (-18 %) and 3 mg/L (-14 %) (Fig. 3b).

Larvae swimming activity in alternating light/dark transitions at 120 hpf also showed an effect of PSNP exposure. During the dark interval, there was an increase in larvae activity at 0.1 and 0.5 mg/L but that was only significant for the later (6 % and 29 % respectively). However, activity decreased by 4 % for larvae exposed to 3 mg/L (Fig. 3c). During the light period there was a decrease in movement for larvae at 0.1 mg/L (-11 %) and an increase at 0.5 mg/L (37 %) and 3 mg/L (11 %) that was only significant for the intermediate concentration.

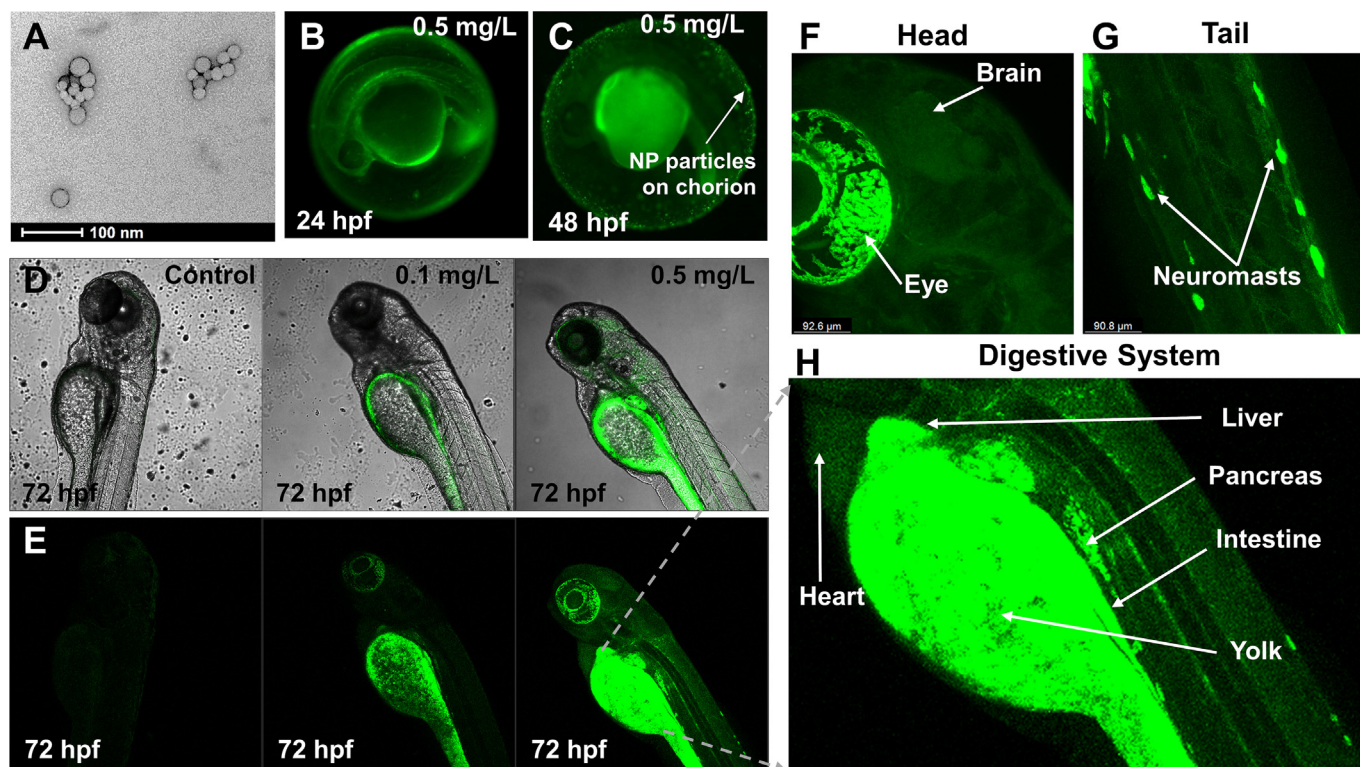


Fig. 1. Accumulation of fluorescent NP in zebrafish larvae. (a) Electron microscope images of nanoparticles in embryo water after sonication. Panels (b) and (c) depict in-chorion accumulation after 24 and 48 hpf at 0.5 mg/L. Panels (d) and (e) show PSNP accumulation in control, 0.1 and 0.5 mg/L exposed larvae after 72 hpf viewed in a combined fluorescent and bright field way (d) or only fluorescent view (e). Close-up of accumulation in eyes and brain (f), neuromasts (lateral line) (g), and digestive system (h).

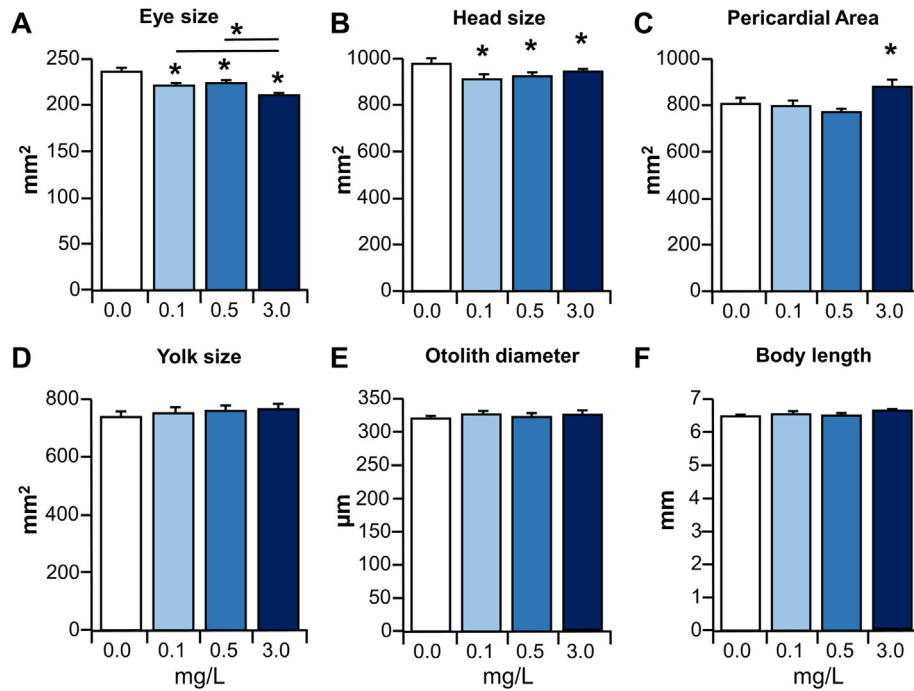


Fig. 2. Eye size (a), head size (b), pericardial area (c), yolk size (d), otolith diameter (e), and body length (f) of larvae exposed to 0.1, 0.5, and 3 mg/L PSNP. Measurements were taken at 72 hpf. Data are presented as means \pm SE. Red asterisk above bar denotes significant difference between treatment and control ($p < 0.05$); black asterisk denotes significant difference among treatments ($p < 0.05$).

Anxiety-like behavior evaluation through the study of thigmotaxis behavior during visual stimulation (dark and light periods) showed that during dark periods (Fig. 4a), larvae exhibited increased anxiety at 0.1 and 0.5 mg/L with less time in the well center (-17 and -30 % respectively) and more time at the edge (8 and 15 %). This trend was also true for the light period although not as pronounced, with less time in the well center (-9 and 10 % respectively) and more near the edge (5 and 6 %) (Fig. 4b). These differences only showed significance for at 0.5 mg/L during the dark period. On the other hand, larvae exposed to the highest PSNP concentration of 3 mg/L showed an opposite trend. During both light and dark periods these larvae spent more time at the well center (~ 15 %) and less at the edge (~ 9 %) than controls which denotes a decrease in anxiety (Figs. 4a and b). Although not significant against controls, 3 mg/L exposed larvae spent significantly more time at the center than the edge than larvae exposed to the two lower concentrations. Interestingly, effects of PSNP on anxiety

caused by auditory stimulation (tapping noises) showed a concentration dependent pattern of anxiolytic effects. Larvae exposed to 0.5 and 3 mg/L exhibited more time in well centers (23 and 40 % respectively; Fig. 4c) and less at the edge (-12 and -21 %), although significant only at 3 mg/L.

In response to a first loud auditory stimulus, larvae exposed to 0.1 and 0.5 mg/L PSNP, presented a significant increase reaction (more distance traveled) during the first jump (~ 26 % more than controls for both; Fig. 5 a, b). However, when exposed to a second “first” stimulus after a 15 min pause, the jump was similar to that of controls. On the other hand, larvae exposed to 3 mg/L exhibited a less intense reaction as they traveled less distance than controls for both “first” tapping noises (-7 and -10 % respectively; Fig. 5c). Interestingly, PSNP did not appear to have an effect on larvae habituation to a series of tapping noises as habituation slopes did not differ at any concentration with respect to controls (Fig. 5).

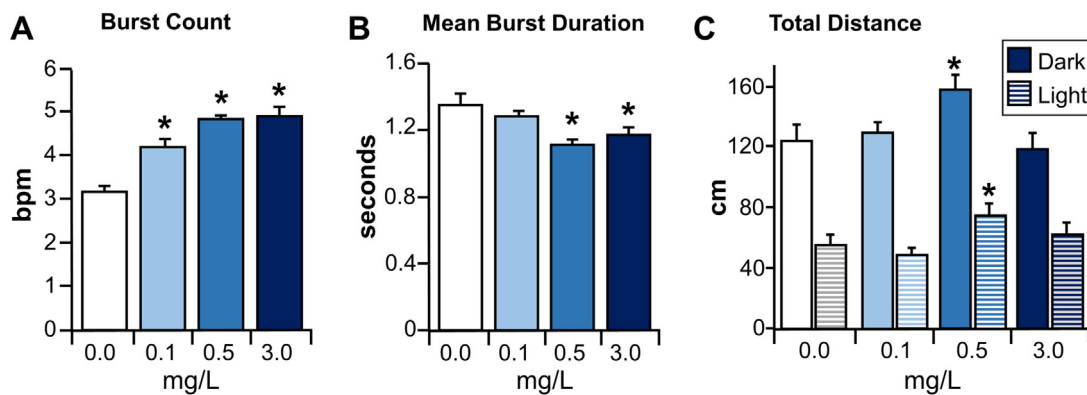


Fig. 3. Embryo (24 hpf) tail bursts per minute (bpm) (a) and burst duration (b); and larvae (120 hpf) total distance traveled (c) after exposure to 0.1, 0.5, and 3 mg/L PSNP. Burst activity was measured in the dark. Distance was measured during dark (solid columns) and light (striped columns) intervals. Data are presented as means \pm SE. Asterisk above bar denotes significant difference between treatment and control ($p < 0.05$).

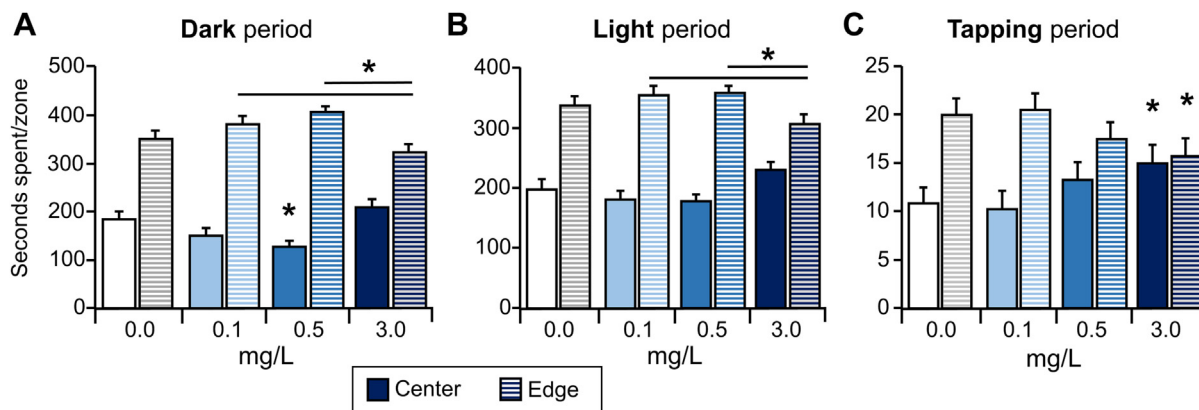


Fig. 4. Seconds spent by 120 hpf larvae in well center (solid columns) and well edge (striped columns) during visual test dark (a) and light (b) periods, and during auditory tapping test (c) after exposure to 0.1, 0.5, and 3 mg/L polystyrene NP. Data are presented as means \pm SE. Red asterisk above bar denotes significant difference between treatment and control ($p < 0.05$). Black asterisk denotes difference between treatments.

3.5. Molecular and enzymatic response after PSNP exposure

We have investigated changes in expression profiles of different genes involved in endocrine related pathways (thyroid, adrenal, and dopamine) in 120 hpf ZF embryos as a result of PSNP exposure. Results show that in general pathways were affected in a dose-dependent manner but direction and relative difference varied depending on each gene studied (Fig. 6). Gene transcripts involved in the hypothalamic–pituitary–thyroid (HTA) axis were affected (Fig. 6a), with significant concentration-dependent downregulation of *trh*, *trhr*, and *tshb*, and significant dose-dependent upregulation of *tshr*, *tra*, and *ugt1ab*. With regards to gene transcripts from the Hypothalamus-pituitary-interrenal (HPA) axis (Fig. 6b), we found significant concentration-dependent upregulation for *crha*, *crhpb*, and *acthb*, and a biphasic response for *crhb*, with significant upregulation at 0.1 and 0.5 mg/L that decreased at 3 mg/L, but continued to be higher than control. Gene transcripts involved in dopamine metabolism were also affected (Fig. 6c), with significant concentration-dependent upregulation of *th1*, and a biphasic response for *drd2a* and *drd2b*, with significant upregulation with respect to control at all doses but with the highest upregulation at 0.5 mg/L.

The acetylcholinesterase enzyme in 120 hpf ZF larvae was altered by PSNP exposure, with an observed generalized decrease of enzymatic activity (Fig. 7). This decrease was significant for all treatments and followed a slight concentration dependent manner with 0.1, 0.5, and 3 mg/L exposed larvae having 18, 19, and 20 % less activity than controls respectively (Fig. 7).

4. Discussion

Nanoplastics are emergent contaminants that are predicted to increase in concentration in all environmental compartments due mainly to degradation of the vast amounts of macroplastics deposited in oceans/landfills since the 1970s, but also by direct emissions of NP in personal care and industrial products (Geyer et al., 2017; Hernandez et al., 2017). Despite technical difficulties, NP have recently been found in environmental compartments such as the ocean, coastal areas, polar ice, freshwater bodies, and the atmosphere (Davranche et al., 2020; Materić et al., 2022a; Materić et al., 2022b; Materić et al., 2022c; Wahl et al., 2021). In a recent work Materić et al. (2022c) found NP in Swedish lakes and streams with an average concentration of 0.56 mg/L. This confirms that NP concentrations used for ZF exposure in the present work are indeed possible to encounter in the environment.

Little is known about potential NP toxic effect mechanisms on aquatic and terrestrial organisms, and human beings. Since MP have been found in several human tissues such as blood, lungs, gastrointestinal tract, and placenta (Gruber et al., 2022; Jenner et al., 2022; Leslie et al., 2022; Ragusa et al., 2021; Schwabl et al., 2019), its only logical to assume NP can be present in human bodies. However, due to analytical difficulties, no data exist yet in this regard. If NP are able to cross the human placenta and blood brain barrier as in vitro and in vivo studies suggest (Aghaei et al., 2022; Hoelting et al., 2013; Hwang et al., 2022; Shan et al., 2022) it is of the utmost importance to evaluate their possible early endocrine and neurotoxic effects. Our study has used a broad battery of assays, from molecular to physiological, including genetic effects, enzymatic, morphological and behavioral assays. Our results show clear PSNP accumulation in most organs and deleterious effects ranging from the organism to the molecular level that are in line with some of those previously observed (Torres-Ruiz et al., 2021; Ullah et al., 2023).

4.1. Nanoplastic characterization

Most NP toxicity studies present the challenge of replicating how NP behave naturally when they are dispersed in different types of media (ocean water, freshwater, etc.). In our case, PSNP characterization by TEM and NTA showed individual particles had size in accordance with commercial specifications (25.1 ± 4 nm) but particles agglomerated over time to a mean size of 100 nm in all concentrations, in spite of thorough sonication (Fig. 1a and Fig. A.1). No attempt was made to correct this particle behavior as the addition of surfactants could confound toxicity measurements (Bruinink et al., 2015; Summers et al., 2018). In addition, agglomeration of particles better represents natural conditions (Alimi et al., 2018; Lins et al., 2022) and it may alter their toxicity. For example, it has been shown that non-agglomerated polystyrene particles were less toxic for the invertebrate *Daphnia magna* (Vaz et al., 2021) but more toxic for the rotifer *Brachionus plicatilis* (Manfra et al., 2017). Different treatments such as sonication or addition of surfactant agents have been used to decrease aggregation (Eitzen et al., 2020). However, agglomerates are likely to be formed again in test medium with time and, once inside the model organism, particular agglomeration/de-agglomeration mechanisms could be occurring in different organs or tissues that could affect toxicity and clearance time (Bruinink et al., 2015). Moreover, the lack of correlation between degree of toxicity and PSNP particle size observed in a review of ZF embryo studies (Torres-Ruiz et al., 2021) could be due to different patterns of agglomeration in different test media. It is clear that future studies should monitor aggregation patterns and include data on this issue in published articles.

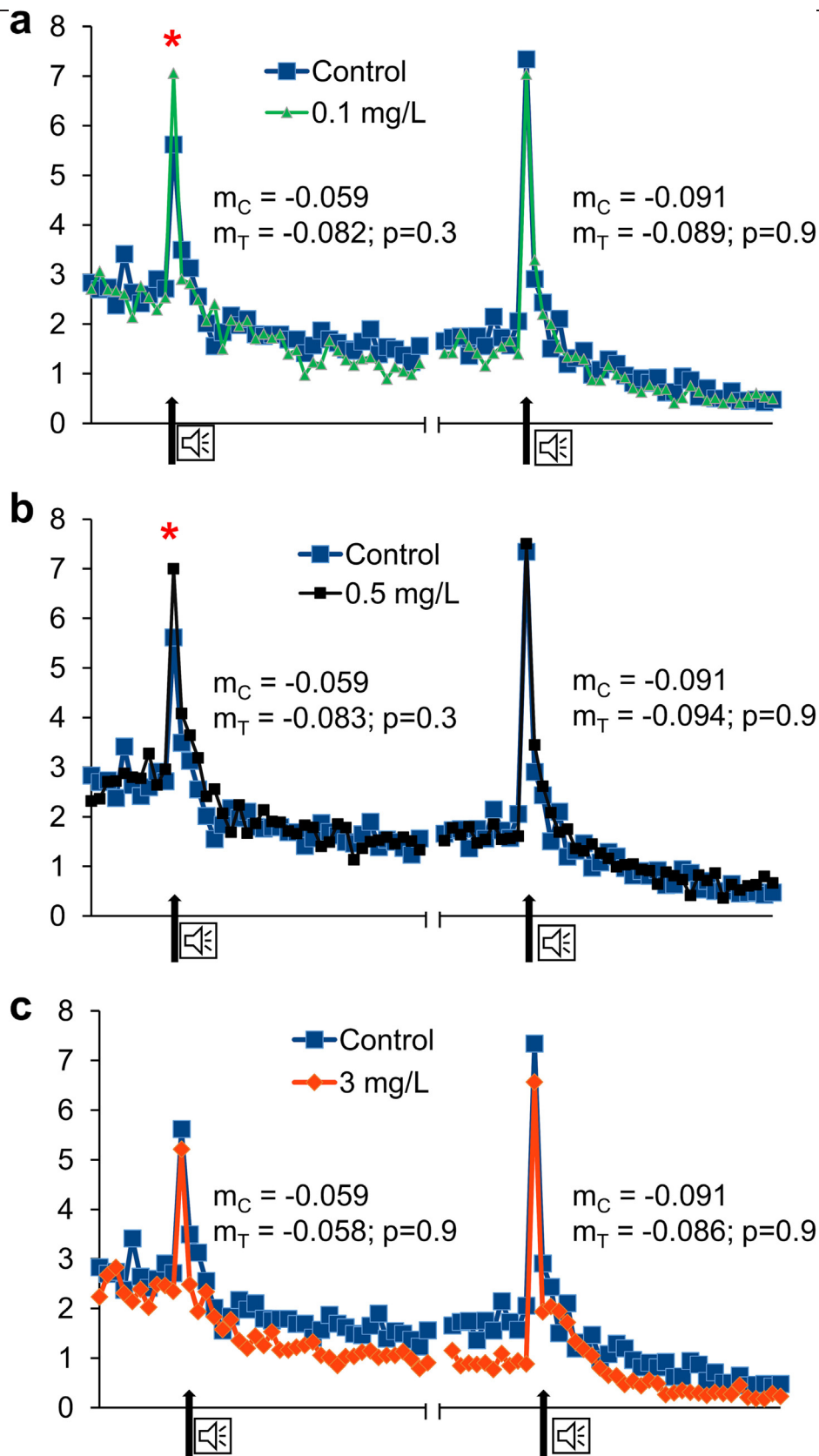


Fig. 5. Distance traveled per second during tapping intervals by 120 hpf larvae exposed to 0.1 mg/L (a; green line), 0.5 mg/L (b; black line), and 3 mg/L (c; orange line) polystyrene NP compared to controls (blue line). Each symbol along a line represents distance traveled in a one second interval. Tapping period starts at black arrow and continues every second for 30 s. After a 15 min pause (x axis break), a second tapping interval starts (second black arrow). Data are presented as means. Slopes of distance traveled/time for each tapping interval were calculated and presented as m_C for control slope and m_T for treatment slope. Asterisk above lines denotes significant differences between treatment and control in specific time points ($p < 0.05$).

4.2. Nanoparticle accumulation

PSNP were observed to accumulate in most organs (Fig. 1). Accumulation started as soon as PSNP were added to the medium and increased from 24 to 72 hpf (Fig. 1 b-d). Embryos protected by the chorion had less overall PSNP fluorescence compared with hatched embryos. This was unexpected since our PSNP size of 30 nm is well below the ZF chorion pore diameter of ~200 nm (Van Pomeran et al., 2017). However, since electron microscopy showed PSNP aggregation, and lumps of PSNP were observed stuck to the chorion, it is clear that it is serving as a protective barrier against PSNP penetration due to an increase in particle effective diameter (Fig. 1c). Nevertheless, embryos at 48 hpf showed fluorescence mainly in the yolk (Fig. 1c) and after hatching (72 hpf) we could observe an increase in PSNP fluorescence in other organs as well (Fig. 1 d, e). As observed before, the yolk had the highest degree of PSNP accumulation, probably selectively aggregating them due to its lipophilic nature. The manner in which NP are able to penetrate the yolk sac epithelium deserves further study, and the ZF is an excellent model as it shares several yolk characteristics with humans over the first weeks of their development (Sant and Timme-Laragy, 2018). NP probably travel from the yolk to the embryo first through the yolk syncytial layer (Osborne et al., 2013) and then through the circulatory system (Hwang et al., 2022) although the exact mechanisms for this remain largely unknown.

The digestive tract was the second most affected by PSNP accumulation (Fig. 2h), with particles observed mostly in the gut, liver, and pancreas, as observed before (Brun et al., 2018; Brun et al., 2019). Accumulation in these organs could come directly from the yolk but also by NP ingestion, after 72 hpf, when embryos' mouths start to function (Van Pomeran et al., 2017). In addition, larvae were observed ejecting PSNP from the anal pore (Video A.1) but this discharge rate was not calculated and deserves further study in order to better understand NP metabolism, toxicokinetics, and clearance rates.

The brain and important sensory organs such as the eyes and lateral line were also shown to accumulate PSNP (Fig. 1f, g). Few studies have shown accumulation of NP in lateral line organs (Brun et al., 2018; Parenti et al., 2019). However, eye accumulation has been frequently observed before in larvae exposed to different PSNP sizes and concentrations (Van Pomeran et al., 2017; Zhang et al., 2020a; Zhang and Goss, 2020). The possibility of NP affecting ZF visual capacity has seldom been studied specifically, although the expression of some eye pigment and retinal system genes have been shown to be affected in exposed larvae (Zhang et al., 2020a; Liu et al., 2022). Accumulation in the larval ZF brain was observed by 44 % studies examining PSNP distribution, and genes and metabolites related to CNS function have been shown to be affected as well (Zhang et al., 2020a; Teng et al., 2022). Moreover, PSNP have been shown to increase nervous system cell apoptosis and affect motor neuron development (Teng et al., 2022; Zhang et al., 2022). Therefore, behavioral changes observed in PSNP exposed larvae (see below) could be a result of PSNP accumulation and disruption of both the central nervous system and sensory organs.

4.3. Morphological and cardiac effects

Few studies have addressed morphological defects as a result of NP exposure (Torres-Ruiz et al., 2021). In this study, body length, curvature, yolk size, and otolith diameter were not affected by PSNP exposure (Fig. 2 d-f). This is in agreement with other studies (Brun et al., 2019) but contrary to others (Chen et al., 2017) using similar concentrations and particle size. On the other hand, we observed a decrease in eye and head size (Fig. 2a, b). Since whole body length was not affected, it is possible that head and sensory organ are especially affected by PSNP exposure. Although head size was only slightly affected, the range of eye size decrement observed has been shown to be important for adaptation in other fish species (Lisney et al., 2020). Potential mechanisms behind these effects could include disruption of neuronal and eye cell proliferation (Hill et al., 2003; Huang et al., 2013) as a result of PSNP accumulation (Fig. 1f). This is

supported by previous ZF studies that have found downregulation of CNS and eye pigment gene expression (Zhang et al., 2020a; Liu et al., 2021a). Future work should consider this as a possible mechanisms underlying NP neurotoxicity.

Another important observed malformation is an increase in heart area with PSNP exposure at the highest concentration caused by cardiac edema (Fig. 2c). However, even though we observed bradycardia due to fluorescent PSNP exposure (Fig. A.3) we could not test this endpoint for the present study due to technical difficulties. Nevertheless, cardiotoxic effects (mainly bradycardia) have been observed before for PSNP exposed ZF (Duan et al., 2020; Hu et al., 2020; Dai et al., 2023). Possible explanations for cardiotoxicity include activation of the hydrocarbon aryl receptor (Shankar et al., 2020), effects on vascular endothelial growth factor system (Dai et al., 2023), or NP accumulation in sarcomeres (Pitt et al., 2018) that elicit a decrease in cardiomyocyte proliferation, as both have been shown to be common cardiotoxicity mechanisms (Chen, 2013; Nguyen and Bradfield, 2008).

4.4. Behavioral effects

Neurotoxic effects of PSNP exposure were evaluated through a series of behavioral endpoints. Our study confirms PSNP are neurotoxic but specific adverse effects were dependent on the behavior studied and development time.

ZF embryos develop a first motor response at about 24 hpf by spontaneous tail bursts generated by primal muscle innervation that have been shown to be a first screen mechanism of developmental neurotoxicity (de Oliveira et al., 2021; Saint-Amant and Drapeau, 1998). Our study measured these coils at 24 hpf \pm 1 h and so they can be considered representative. Results show PSNP had an effect on tail coiling activity, with a concentration dependent increase in burst counts per minute but a decrease in burst duration (Fig. 3a, b). Hyperactivity was also observed during the light/dark locomotor response test at 120 hpf but only at the two lowest concentrations, with a decrease of activity at 3 mg/L, showing that increasing the duration of exposure caused larvae to switch activity patterns. Considering several genes, involving oxidative stress, cell death, and hormonal balance were specially altered at this concentration at 120 hpf (Martin-Folgar et al., 2023, Figs. 3, 5, 6), it is clear that this decrease in movement implies a greater effect of PSNP toxicity. In addition, even though we did not test higher concentrations for the present work, a preliminary study done for dose-ranging (results not shown) revealed that a concentration of 5 mg/L caused larvae to be practically immobile. Taken together, these results suggest a gradual increase of activity at intermediate concentrations that then progressively decreases to severe hypoactivity. This type of hormetic response is typical of endocrine disruption (Martínez et al., 2019) and could explain why both hypoactivity and hyperactivity have been found in previous studies of NP effects (Torres-Ruiz et al., 2021; Manuel et al., 2022). Alterations in carbohydrate and cortisol metabolism caused by PSNP have been proposed as possible explanations for hyperactivity (Brun et al., 2019; Faught and Vijayan, 2021) but disruption of neuromotor control pathways could also play a role (Pedersen et al., 2020; Zhang et al., 2022). On the other hand, the generalized hypoactivity observed at the highest concentration could be due to increase brain PSNP accumulation that could cause major alterations at the molecular and cellular levels, causing overall cytotoxicity and brain cell apoptosis (Chen et al., 2017; Hu et al., 2020; Teng et al., 2022). Further evidence of this is found in our previous work (Martin-Folgar et al., 2023) in which we found genes encoding for superoxide dismutase (*sod 1* and *2*), apoptotic genes (*cas 1* and *8*), and interleukin 1- β (*il1 β*) were highly activated at the concentration of 3 mg/L, suggesting overall increase in cellular stress at this concentration. A possible mechanism of toxicity influencing behavioral alterations is acetylcholinesterase (AChE) inhibition. In this study (Fig. 7) and in a previous gene expression study (Martin-Folgar et al., 2023) we have found a decrease in AChE at all concentrations. Therefore, the decrease in mRNA expression correlates with a decrease in protein activity. It is possible that, together with other molecular mechanisms, AChE inhibition is

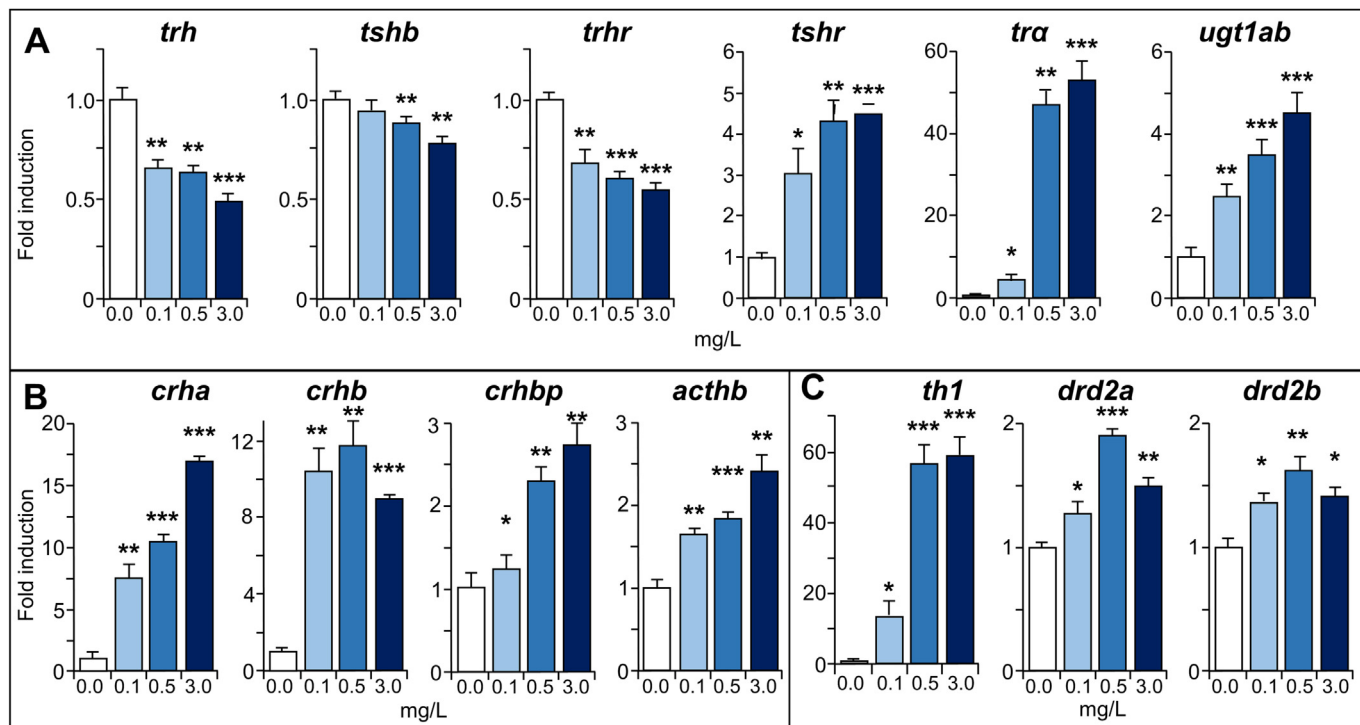


Fig. 6. Expression profiles of genes related to the HPT axis (a), the HPA axis (b), and dopamine metabolism (c). Data are presented as mean fold difference with respect to controls \pm SE. Asterisk above bar denotes significant difference between treatment and control ($p < 0.05$).

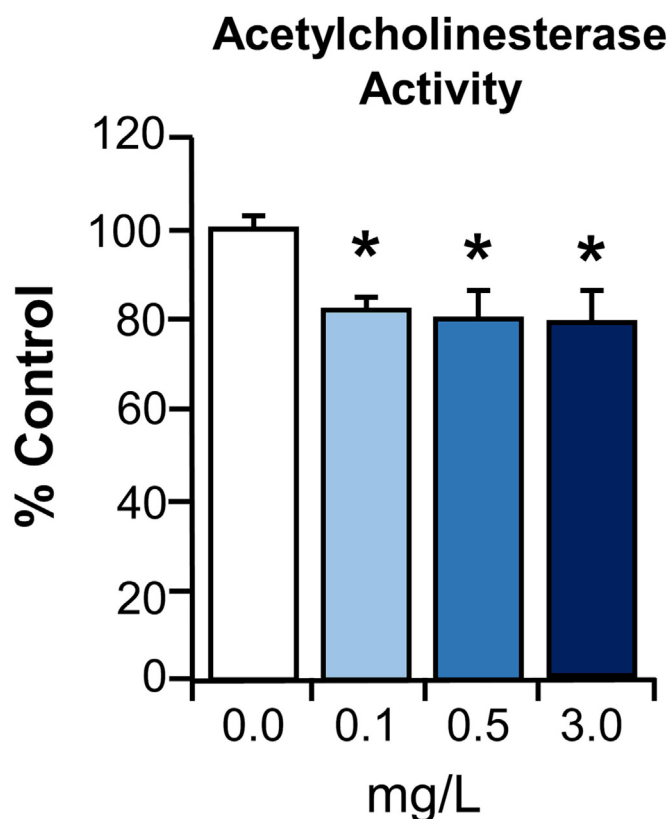


Fig. 7. Acetylcholinesterase activity of 120 hpf larvae exposed to 0.1, 0.5, and 3 mg/L PSNP. Data are presented as mean percent with respect to controls \pm SE. Asterisk above bar denotes significant difference between treatment and control ($p < 0.05$).

part of what is causing hyperactivity at lower concentrations. However, effects on AchE could be interacting with other possible mechanisms such as disruption of dopamine metabolism. Dopamine agonists have been shown to induce hyperactivity in mice and ZF, presenting a biphasic response (Ek et al., 2016). Our results show upregulation of a gene involved in dopamine production (*th1*) and the dopamine receptors *drd2a* and *drd2b* (Fig. 6c), that could be contributing to the hyperactive phenotype. Alterations in dopaminergic metabolites have been observed before in relation to behavioral alterations in ZF embryos exposed to PSNP (Hwang et al., 2022) but in this work no genetic changes were observed. In addition, contribution of other factors such as hormone-related imbalances could also play a role in the activity patterns observed (see below).

In regards to anxiety related effects, our study is the first to assess consequences of PSNP exposure on thigmotaxis behavior in ZF larvae, in response to visual and auditory stimuli. This wall hugging innate response is a measure of anxiety and has been used extensively to study rodent response to anxiolytic and anxiogenic drugs/toxicants (Estrela et al., 2021; Karl et al., 2003; Prut and Belzung, 2003). Moreover, it has also been shown to be a reliable anxiety-like behavior measurement in the ZF embryo model (Schnörr et al., 2012), and recently also in humans (Gromer et al., 2021). The central assumption for this endpoint is that larvae avoid the center of the well (open space) due to an innate fear of predators and prefer to move along the edges, especially during stress periods. Results from this study show that response depended on type of stimulus. PSNP elicited an anxiogenic effect in response to visual stimuli at low and intermediate concentrations but anxiolytic effects at the highest concentration (Fig. 4a, b), contrary to effects observed by Manuel et al. (2022) who observed a decrease in anxiety at concentrations higher than 0.1 mg/L. This type of response has been shown for some drugs with contrasting effects of visual thigmotaxis depending on concentration. For example, the serotonergic drug 3,4-methylenedioxymethamphetamine (MDMA) causes anxiogenic effects at lower concentrations and anxiolytic effects at higher concentrations (Lin et al., 1999). Moreover, these results are in line with results observed for the light/dark locomotion assay, so it could be concluded that PSNP elicited hyperactivity combined with increased anxiety at the lower concentrations and hypoactivity and lower anxiety at the highest concentration. On the

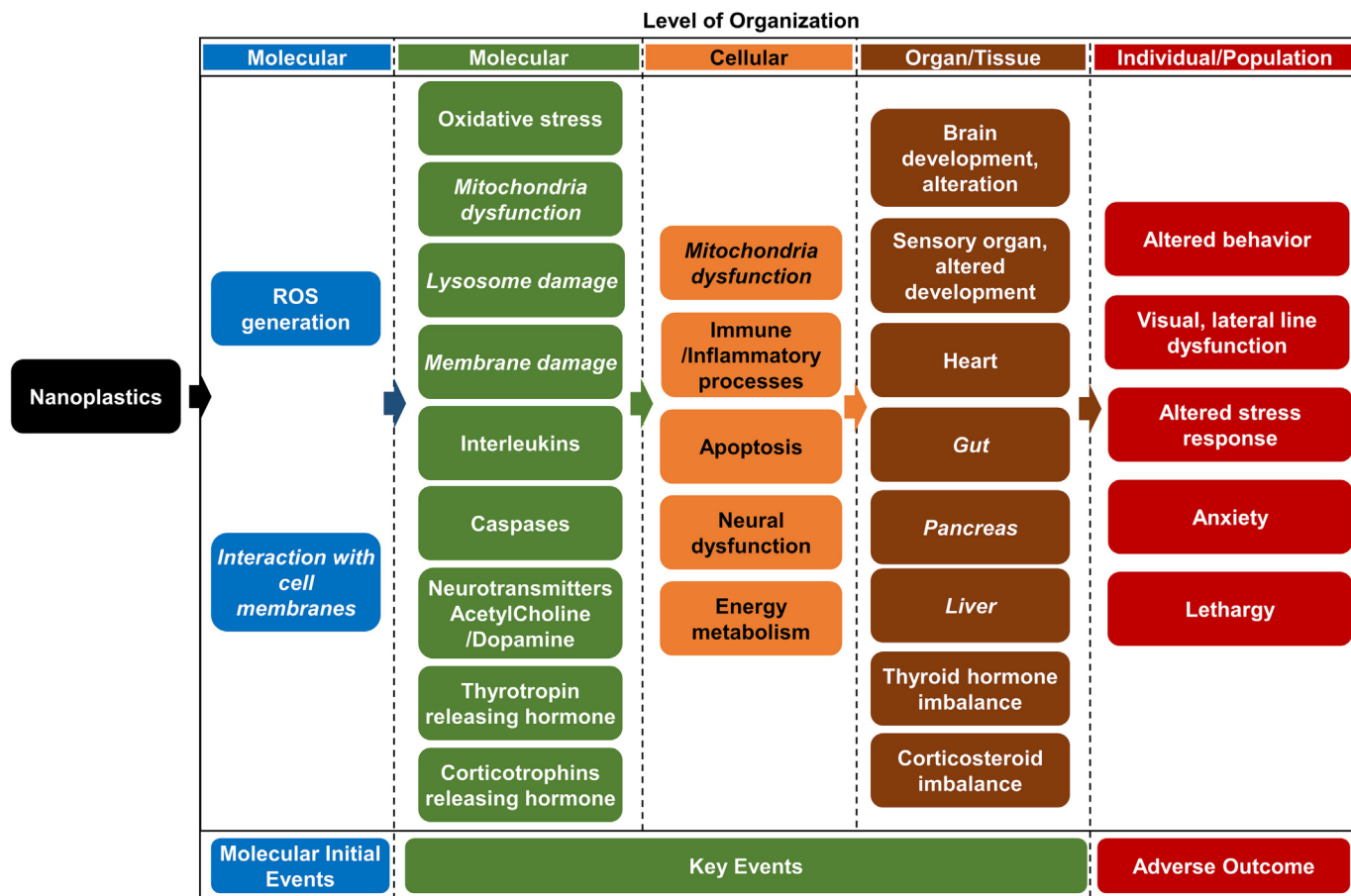


Fig. 8. Proposed adverse outcome pathway for NP toxicity related to endocrine and neurotoxic effects. KE: key event. AO: adverse outcome. Events in italics were not tested directly by authors.

other hand, in response to auditory stimuli, PSNP had an anxiolytic effect that was dose dependent (Fig. 4c). Even though few studies have ever compared thigmotaxis effects due to both visual and auditory cues, a study with rats revealed this behavior can differ in response to different stimuli, with rats exposed to noise spending less time in the center than rats exposed to light only (Hirsjarvi and Junnila, 1986).

Another measure of anxiety is the startle response: This reflex behavior is shared by all vertebrates and is related to activation of brainstem motor neurons by Mauthner cells in ZF or similar neurons in the caudal pontine reticular formation in humans (Eaton et al., 2001; Weber et al., 2008). It has been a model for sensorimotor response, anxiety, and attention in many species due to its translational value (Fendt and Koch, 2013). Moreover, its defects are related to human neurological disorders such as anxiety, attention deficit or schizophrenia (Fetcho and McLean, 2009; Poli and Angrilli, 2015). Our results show that larvae exposed to the two lower PSNP concentrations had a higher startle response than controls (Fig. 5a, b) whereas larvae exposed to the highest concentration had a diminished response (Fig. 5c). Therefore, at these two lower PSNP concentrations, larvae that were more anxious, according to visual thigmotaxis experiment, responded with a stronger startle. However, at the highest concentration, 120 hpf larvae seem to have an overall decrease in movement, anxiety, and startle response, and in this case PSNP are mimicking a sedative more than an anxiolytic drug (Schallek and Schlosser, 1979). Interestingly, when comparing startle behavior with thigmotaxis in response to sound, the pattern is not similar for the two lower concentrations. Possible explanations include different neuronal pathways controlling both responses that could be affected differentially by PSNP. In addition, lateral line disruption by PSNP cannot be ruled out due to particular accumulation in neuromasts observed (Fig. 1g).

Habituation is a form of early learning exhibited by all vertebrates, and consists on reduced reaction to repeated stimuli (Roberts et al., 2016). In ZF, habituation has been linked to the *N*-methyl-D-aspartate (NMDA) receptor and protein synthesis, and toxicants can affect how larvae modulate this response (Best et al., 2008; Roberts et al., 2011). In this study, we found no evidence of PSNP effects on habituation (Fig. 5), despite disruption in locomotion and anxiety responses.

4.5. Hormone disruption effects

In order to assess possible endocrine disruption effects of PSNP we have examined transcription of genes related to the HPT and HPA axes. The HPT axis is an important feedback control in the neuroendocrine system responsible for the regulation of thyroid hormones that in turn regulate metabolism and stress response (Hoermann et al., 2015). On the other hand, the HPA axis regulates glucocorticoid, epinephrine and norepinephrine production and thus is important in stress control but also in other body processes such as digestion, immune system, energy use, and sexuality (Rey et al., 2008). Our study shows that both pathways were affected by PSNP exposure albeit in different degrees and directions depending on specific genes (Fig. 6a, b).

Genes related to thyroid function were affected by down regulation at the level of hypothalamus (*trh*), and pituitary (*trhr* and *tshb*), and up regulation at thyroid (*tshr*) and thyroid hormone metabolism in target tissues (*thra*, *ugt1ab*) levels (Fig. 6a). This implies an overall alteration of the HPT axis that could result in an imbalance of thyroid hormone metabolism similarly to those observed before in NP exposed ZF and rats (Amereh et al., 2019; Zhao et al., 2020). In the present study, this could be part of the reason for some of the observed phenotypes such

as decreased eye or head size (Baumann et al., 2016; Fang et al., 2022). In addition, it could be contributing to altered behavioral phenotypes, as hyperactivity has been shown before in ZF with unbalanced thyroid hormone levels (Walter et al., 2019).

Genes related to the HPA axis were affected mainly by upregulation of *crha* and *crhb* at the hypothalamus and upregulation of *acthb* at the pituitary (Fig. 6b). In addition, we also observed upregulation of *crhbp*, thought to regulate bioavailability of Corticotropin Releasing Hormone (CRH) (Westphal and Seasholtz, 2006). These effects could be partly responsible for hyperactivity and altered anxiety responses observed as increased cortisol levels have been shown to induce hyperactive phenotypes in NP exposed ZF (Amereh et al., 2019; Brun et al., 2019; Walter et al., 2019). Future studies should consider the potential role of NP contamination in the increase levels of anxiety and depression observed in the overall human population in recent years as it has been proposed that anxiety problems are related to environmental pollution and NP could potentially be part of this problem (da Costa Araújo and Malafaia, 2021; Trushna et al., 2021).

4.6. NP adverse outcome pathway

Our study has been the first to combine a battery of behavioral assays with endocrine disruption markers to assess potential NP toxicity. Our present results clearly show that even in an aggregated form and at low concentrations, these toxicants can alter hormonal homeostasis that could result, in combination with neurotransmitter disturbances, in observed hyperactive and anxious phenotypes at low concentrations. In combination with our previous results (Martin-Folgar et al., 2023), we propose an adverse outcome pathway (AOP) for NP toxicity (Fig. 8). Polystyrene NP AOP would start with molecular initiating events such as the physical disruption of membranes that could cause organelle damage and of particular importance, lysosome and mitochondrial damage (Matthews et al., 2021; Yang and Wang, 2023). This would generate oxidative stress (i.e. ROS production) that could induce the activation of antioxidant mechanisms (i.e. SOD, catalases) and increased interleukin and caspase production (i.e. interleukin 1- β , caspases 1 and 8) (Martin-Folgar et al., 2023). In addition, molecular events in the CNS could include an effect on neurotransmitters (i.e. acetylcholine, dopamine, Figs. 6, 7) and brain-produced hormones (i.e. TSH, CRH, Fig. 6). At the cellular level, this would translate in increased inflammation and cell death by apoptosis (Teng et al., 2022), neuronal dysfunction, and/or altered energy metabolism (Manuel et al., 2022). At the organ/tissue level, the above mechanisms could cause altered brain or sensory organ development, hormonal imbalances, and heart abnormalities. In addition, other organs such as pancreas or liver could also be affected considering PSNP accumulation (Fig. 1h) and previous literature findings of hepatic inflammation (Cheng et al., 2022). At the whole organism level, the present study has observed altered behaviors such as increased activity and anxiety at lower doses and lethargy at a high dose. The effects on these behaviors could be due to a variety of complex mechanisms ranging from sensory organ and CNS effects to others such as hormonal imbalances or altered energy metabolism.

This predicted AOP is similar to others proposed for NP toxicity, especially in regards to ROS production as a molecular initiating event, activation of the immune system, and energy metabolism alterations (Hu and Palić, 2020; Liu et al., 2021c). Whole organism effects in AOPs have been proposed to range from growth inhibition to developmental abnormalities (Liu et al., 2021c) to behavioral changes, such as the ones observed in the present work and other works reviewed in Hu and Palić, 2020. However, our study is the first to show endocrine disruption as part of potential molecular initiating events in PSNP induced adverse outcome.

Our study has shown that PSNP can have important toxic effects even in an aggregated form. Considering the concentration of these toxicants are predicted to increase considerably in the next years (Lebreton et al., 2019), it is crucial to continue investigating their mechanisms of action and potential health effects. Even though this study centered in endocrine-related and neurotoxic effects, it is clear that PSNP can

accumulate in other organs and could also affect them. Future studies should consider their relation to important human diseases that have increased in incidence in the last few years such as autism or hyperactivity disorders, anxiety, depression, neurodegenerative processes, and metabolic diseases, among others.

Supplementary data to this article can be found online at <https://doi.org/10.1016/j.scitotenv.2023.162406>.

CRediT authorship contribution statement

All authors contributed to the conception and design of the study.

Monica Torres-Ruiz: Conceptualization, methodology, formal analysis, research, writing, preparation of the original draft, review and editing.

Mercedes de Alba: Methodology, formal analysis, research, review and editing.

Monica Morales: Methodology, formal analysis, research, review and editing.

Raquel Martín-Folgar: Methodology, formal analysis, research, review and editing.

M^{ra}. Carmen González: Methodology, formal analysis, research, review and editing.

Ana I. Cañas-Portilla: Conceptualization, methodology, formal analysis, research, writing, review, editing, and supervision.

Antonio De la Vieja: Conceptualization, methodology, formal analysis, research, writing, review, editing, and supervision.

Data availability

Data will be made available on request.

Declaration of competing interest

The authors declare that they have no known competing financial interests or personal relationships that could have appeared to influence the work reported in this paper.

Acknowledgments

We thank Mari Paz Lopez-Molina and Ana Montero Calle for laboratory technical assistance and Diego Megias for confocal microscopy assistance.

Funding

This work was supported by the Joint Research Institute IMIENS (Grant Number: IMIENS-2020-001-PIC), and the Spanish Government (Grant Number: PID2021-125948OB-I00 from MCIN/AEI/10.13039/501100011033/FEDER, UE to ADV).

References

- Aghaei, Z., Sled, J.G., Kingdom, J.C., Baschat, A.A., Helm, P.A., Jobst, K.J., et al., 2022. Maternal exposure to polystyrene micro-and nanoplastics causes fetal growth restriction in mice. *Environ. Sci. Technol. Lett.* <https://doi.org/10.1021/acs.estlett.2c00186>.
- Alimi, O.S., Farmer, Budarz J., Hernandez, L.M., Tufenkji, N., 2018. Microplastics and nanoplastics in aquatic environments: aggregation, deposition, and enhanced contaminant transport. *Environ. Sci. Technol.* 52, 1704–1724. <https://doi.org/10.1021/acs.est.7b05559>.
- Amereh, F., Eslami, A., Fazelipour, S., Rafiee, M., Zibaii, M.I., Babaei, M., 2019. Thyroid endocrine status and biochemical stress responses in adult male Wistar rats chronically exposed to pristine polystyrene nanoplastics. *Toxicol. Res. (Camb)* 8, 953–963. <https://doi.org/10.1039/C9TX00147F>.
- Andrady, A.L., 2017. The plastic in microplastics: a review. *Mar. Pollut. Bull.* 119, 12–22. <https://doi.org/10.1016/j.marpolbul.2017.01.082>.
- Baumann, L., Ros, A., Rehberger, K., Neuhaus, S.C., Segner, H., 2016. Thyroid disruption in zebrafish (*Danio rerio*) larvae: different molecular response patterns lead to impaired eye development and visual functions. *Aquat. Toxicol.* 172, 44–55. <https://doi.org/10.1016/j.aquatox.2015.12.015>.
- Best, J.D., Berghmans, S., Hunt, J.J.F.G., Clarke, S.C., Fleming, A., Goldsmith, P., et al., 2008. Non-associative learning in larval zebrafish. *Neuropsychopharmacology* 33, 1206–1215. <https://doi.org/10.1038/sj.npp.1301489>.

- Bhagat, J., Zang, L., Nishimura, N., Shimada, Y., 2020. Zebrafish: an emerging model to study microplastic and nanoplastic toxicity. *Sci. Total Environ.* 728, 138707. <https://doi.org/10.1016/j.scitotenv.2020.138707>.
- Bourdineaud, J.P., Rossignol, R., Br ethes, D., 2013. Zebrafish: a model animal for analyzing the impact of environmental pollutants on muscle and brain mitochondrial bioenergetics. *Int. J. Biochem. Cell Biol.* 45, 16–22. <https://doi.org/10.1016/j.biocel.2012.07.021>.
- Bruinink, A., Wang, J., Wick, P., 2015. Effect of particle agglomeration in nanotoxicology. *Arch. Toxicol.* 89, 659–675. <https://doi.org/10.1007/s00204-015-1460-6>.
- Brun, N.R., Koch, B.E.V., Varela, M., Peijnenburg, W.J.G.M., Spalink, H.P., Vijver, M.G., et al., 2018. Nanoparticles induce dermal and intestinal innate immune system responses in zebrafish embryos. *Environ. Sci. Nano* 5, 904–916. <https://doi.org/10.1039/c8en00002f>.
- Brun, N.R., van Hage, P., Hunting, E.R., Haramis, A.G., Vink, S.C., Vijver, M.G., et al., 2019. Polystyrene nanoplastics disrupt glucose metabolism and cortisol levels with a possible link to behavioural changes in larval zebrafish. *Commun. Biol.* 2, 1–9. <https://doi.org/10.1038/s42003-019-0629-6>.
- Chae, Y., An, Y.J., 2017. Effects of micro- and nanoplastics on aquatic ecosystems: current research trends and perspectives. *Mar. Pollut. Bull.* 124, 624–632. <https://doi.org/10.1016/j.marpolbul.2017.01.070>.
- Chae, Y., An, Y.J., 2020. Nanoplastic ingestion induces behavioral disorders in terrestrial snails: trophic transfer effects via vascular plants. *Environ. Sci. Nano* 7, 975–983. <https://doi.org/10.1039/c9en01333k>.
- Chang, X., Xue, Y., Li, J., Zou, L., Tang, M., 2020. Potential health impact of environmental micro- and nanoplastics pollution. *J. Appl. Toxicol.* 40, 4–15. <https://doi.org/10.1002/jat.3915>.
- Chen, J., 2013. Impaired cardiovascular function caused by different stressors elicits a common pathological and transcriptional response in zebrafish embryos. *Zebrafish* 10, 389–400. <https://doi.org/10.1089/zeb.2013.0875>.
- Chen, Q., Gundlach, M., Yang, S., Jiang, J., Velki, M., Yin, D., et al., 2017. Quantitative investigation of the mechanisms of microplastics and nanoplastics toward zebrafish larvae locomotor activity. *Sci. Total Environ.* 584–585, 1022–1031. <https://doi.org/10.1016/j.scitotenv.2017.01.156>.
- Cheng, H., Duan, Z., Wu, Y., Wang, Y., Zhang, H., Shi, Y., et al., 2022. Immunotoxicity responses to polystyrene nanoplastics and their related mechanisms in the liver of zebrafish (*Danio rerio*) larvae. *Environ. Int.* 161, 107128. <https://doi.org/10.1016/j.envint.2022.107128>.
- da Costa Araújo, A.P., Malafaia, G., 2021. Microplastic ingestion induces behavioral disorders in mice: a preliminary study on the trophic transfer effects via tadpoles and fish. *J. Hazard. Mater.* 401, 123263. <https://doi.org/10.1016/j.jhazmat.2020.123263>.
- d'Amora, M., Giordani, S., 2018. The utility of zebrafish as a model for screening developmental neurotoxicity. *Front. Neurosci.* 12, 976. <https://doi.org/10.3389/fnins.2018.00976>.
- Dai, L., Luo, J., Feng, M., Wang, M., Zhang, J., Cao, X., et al., 2023. Nanoplastics exposure induces vascular malformation by interfering with the VEGFA/VEGFR pathway in zebrafish (*Danio rerio*). *Chemosphere* 312, 137360. <https://doi.org/10.1016/j.chemosphere.2022.137360>.
- Davranche, M., Lory, C., Juge, C.L., Blanco, F., Dia, A., Grassl, B., et al., 2020. Nanoplastics on the coast exposed to the North Atlantic gyre: evidence and traceability. *NanoImpact* 20, 100262. <https://doi.org/10.1016/j.impact.2020.100262>.
- Deville, S., Penjweini, R., Smisdom, N., Notelaers, K., Nelissen, I., Hooyberghs, J., et al., 2015. Intracellular dynamics and fate of polystyrene nanoparticles in A549 lung epithelial cells monitored by image (cross-) correlation spectroscopy and single particle tracking. *Biochim. Biophys. Acta* 1853, 2411–2419. <https://doi.org/10.1016/j.bbamcr.2015.07.004>.
- Duan, Z., Duan, X., Zhao, S., Wang, X., Wang, J., Liu, Y., et al., 2020. Barrier function of zebrafish embryonic chorions against microplastics and nanoplastics and its impact on embryo development. *J. Hazard. Mater.* 395, 122621. <https://doi.org/10.1016/j.jhazmat.2020.122621>.
- Eaton, R.C., Lee, R.K.K., Foreman, M.B., 2001. The mauthner cell and other identified neurons of the brainstem escape network of fish. *Prog. Neurobiol.* 63, 467–485. [https://doi.org/10.1016/S0301-0082\(00\)00047-2](https://doi.org/10.1016/S0301-0082(00)00047-2).
- Eitzen, L., Ruhl, A.S., Jekel, M., 2020. Particle size and pre-treatment effects on polystyrene microplastic settlement in water: implications for environmental behavior and ecotoxicological tests. *Water* 12, 3436. <https://doi.org/10.3390/w12123436>.
- Ek, F., Malo, M., Åberg Andersson, M., Wedding, C., Kronborg, J., Svensson, P., et al., 2016. Behavioral analysis of dopaminergic activation in zebrafish and rats reveals similar phenotypes. *ACS Chem Neurosci* 7, 633–646. <https://doi.org/10.1021/acscchemneuro.6b00014>.
- Estrela, F.N., Guimarães, A.T.B., Araújo, A.P.D.C., Silva, F.G., Luz, T.M.D., Silva, A.M., et al., 2021. Toxicity of polystyrene nanoplastics and zinc oxide to mice. *Chemosphere* 271, 129476. <https://doi.org/10.1016/j.chemosphere.2020.129476>.
- Fang, Y., Wan, J.-P., Zhang, R.-J., Sun, F., Yang, L., Zhao, S., et al., 2022. Thyroid Peroxidase Knockout in Zebrafish Recapitulates the Clinical Manifestations of Congenital Hypothyroidism and Reveals Thyroid Hormone Function to Maintain Glucose Homeostasis. <https://doi.org/10.2139/ssrn.4021894> SSRN; 3988615.
- Faria, M., Prats, E., Novoa-Luna, K.A., Bedrossiantz, J., Gómez-Canela, C., Gómez-Oliván, L.M., et al., 2019. Development of a vibrational startle response assay for screening environmental pollutants and drugs impairing predator avoidance. *Sci. Total Environ.* 650, 87–96. <https://doi.org/10.1016/j.scitotenv.2018.08.421>.
- Faught, E., Vijayan, M., 2021. Coordinated action of CRH and cortisol shapes acute stress-induced behavioural response in zebrafish. *Neuroendocrinology* 112, 74–87. <https://doi.org/10.1159/000514778>.
- Fendt, M., Koch, M., 2013. Translational value of startle modulations. *Cell Tissue Res.* 354, 287–295. <https://doi.org/10.1007/s00441-013-1599-5>.
- Fetcho, J.R., McLean, D.L., 2009. Startle response. In: Squire, L.R. (Ed.), *Encyclopedia of Neuroscience*. Academic Press, Oxford, pp. 375–379. <https://doi.org/10.1016/B978-008045046-9.01973-2>.
- Gallego-Urrea, J.A., Tuoriniemi, J., Pallander, T., Hassel ov, M., 2010. Measurements of nanoparticle number concentrations and size distributions in contrasting aquatic environments using nanoparticle tracking analysis. *Environ. Chem.* 7, 67–81. <https://doi.org/10.1071/EN09114>.
- Geyer, R., Jambeck, J.R., Law, K.L., 2017. Production, use, and fate of all plastics ever made. *Sci. Adv.* 3, e1700782. <https://doi.org/10.1126/sciadv.1700782>.
- Gigault, J., Ter Halle, A., Baudrimont, M., Pascal, P.-Y., Gauffre, F., Phi, T.-L., et al., 2018. Current opinion: what is a nanoplastic? *Environ. Pollut.* 235, 1030–1034. <https://doi.org/10.1016/j.envpol.2018.01.024>.
- Gromer, D., Kiser, D.P., Pauli, P., 2021. Thigmotaxis in a virtual human open field test. *Sci. Rep.* 11, 6670. <https://doi.org/10.1038/s41598-021-85678-5>.
- Gruber, E.S., Stadlbauer, V., Pichler, V., Resch-Fauster, K., Todorovic, A., Meisel, T.C., et al., 2022. To waste or not to waste: questioning potential health risks of micro- and nanoplastics with a focus on their ingestion and potential carcinogenicity. *Expos. Health* 1–19. <https://doi.org/10.1007/s12403-022-00470-8>.
- Hernandez, L.M., Yousefi, N., Tufenkji, N., 2017. Are there nanoplastics in your personal care products? *Environ. Sci. Technol. Lett.* 4, 280–285. <https://doi.org/10.1021/acs.estlett.7b00187>.
- Hill, A., Howard, C.V., Strahle, U., Cossins, A., 2003. Neurodevelopmental defects in zebrafish (*Danio rerio*) at environmentally relevant dioxin (TCDD) concentrations. *Toxicol. Sci.* 76, 392–399. <https://doi.org/10.1093/toxsci/kfg241>.
- Hirsjarvi, P.A., Junnila, M.A., 1986. Effects of light and noise test stimuli on the open-field behavior of wistar rats. *Scand. J. Psychol.* 27, 311–319. <https://doi.org/10.1111/j.1467-9450.1986.tb01209.x>.
- Hoelting, L., Scheinhardt, B., Bondarenko, O., Schildknecht, S., Kapitzka, M., Tanavde, V., et al., 2013. A 3-dimensional human embryonic stem cell (hESC)-derived model to detect developmental neurotoxicity of nanoparticles. *Arch. Toxicol.* 87, 721–733. <https://doi.org/10.1007/s00204-012-0984-2>.
- Hoermann, R., Midgley, J.E.M., Larisch, R., Dietrich, J.W., 2015. Homeostatic control of the thyroid-pituitary Axis: perspectives for diagnosis and treatment. *Front. Endocrinol. (Lausanne)* 6. <https://doi.org/10.3389/fendo.2015.00177>.
- Howe, K., Clark, M.D., Torroja, C.F., Torrance, J., Bertelot, C., Muffato, M., et al., 2013. The zebrafish reference genome sequence and its relationship to the human genome. *Nature* 496, 498–503. <https://doi.org/10.1038/nature12111>.
- Hu, Q., Wang, H., He, C., Jin, Y., Fu, Z., 2020. Polystyrene nanoparticles trigger the activation of p38 MAPK and apoptosis via inducing oxidative stress in zebrafish and macrophage cells. *Environ. Pollut.* 269, 116075. <https://doi.org/10.1016/j.envpol.2020.116075>.
- Huang, L., Wang, C., Zhang, Y., Wu, M., Zuo, Z., 2013. Phenanthrene causes ocular developmental toxicity in zebrafish embryos and the possible mechanisms involved. *J. Hazard. Mater.* 261, 172–180. <https://doi.org/10.1016/j.jhazmat.2013.07.030>.
- Hwang, K.S., Son, Y., Kim, S.S., Shin, D.S., Lim, S.H., Yang, J.Y., et al., 2022. Size-dependent effects of polystyrene nanoparticles (PS-NPs) on behaviors and endogenous neurochemicals in zebrafish larvae. *Int. J. Mol. Sci.* 23. <https://doi.org/10.3390/ijms231810682>.
- Jenner, L.C., Rotchell, M., Bennett, R.T., Cowen, M., Tentzeris, V., Sadofsky, L.R., 2022. Detection of microplastics in human lung tissue using μ FTIR spectroscopy. *Sci. Total Environ.* 831, 154907. <https://doi.org/10.1016/j.scitotenv.2022.154907>.
- Jeong, B., Baek, J.Y., Koo, J., Park, S., Ryu, Y.K., Kim, K.S., et al., 2022. Maternal exposure to polystyrene nanoplastics causes brain abnormalities in progeny. *J. Hazard. Mater.* 426, 127815. <https://doi.org/10.1016/j.jhazmat.2021.127815>.
- Karl, T., Pabst, R., von H orsten, S., 2003. Behavioral phenotyping of mice in pharmacological and toxicological research. *Exp. Toxicol. Pathol.* 55, 69–83. <https://doi.org/10.1078/0940-2993-00301>.
- Kik, K., Bukowska, B., Sicińska, P., 2020. Polystyrene nanoparticles: sources, occurrence in the environment, distribution in tissues, accumulation and toxicity to various organisms. *Environ. Pollut.* 262, 114297. <https://doi.org/10.1016/j.envpol.2020.114297>.
- Kimmel, C.B., Patterson, J., Kimmel, R.O., 1974. The development and behavioral characteristics of the startle response in the zebra fish. *Dev. Psychobiol.* 7, 47–60. <https://doi.org/10.1002/dev.420070109>.
- K uster, E., 2005. Cholin- and carboxylesterase activities in developing zebrafish embryos (*Danio rerio*) and their potential use for insecticide hazard assessment. *Aquat. Toxicol.* 75, 76–85. <https://doi.org/10.1016/j.aquatox.2005.07.005>.
- Lebreton, L., Egger, M., Slat, B., 2019. A global mass budget for positively buoyant macroplastic debris in the ocean. *Sci. Rep.* 9, 12922. <https://doi.org/10.1038/s41598-019-49413-5>.
- Lehner, R., Weder, C., Petri-Fink, A., Rothen-Rutishauser, B., 2019. Emergence of nanoplastic in the environment and possible impact on human health. *Environ. Sci. Technol.* 53, 1748–1765. <https://doi.org/10.1021/acs.est.8b05512>.
- Leslie, H.A., van Velzen, M.J.M., Brandsma, S.H., Vethaak, A.D., Garcia-Vallejo, J.J., Lamoree, M.H., 2022. Discovery and quantification of plastic particle pollution in human blood. *Environ. Int.* 163, 107199. <https://doi.org/10.1016/j.envint.2022.107199>.
- Letcher, T.M., 2020. Plastic waste and recycling: environmental impact. *Societal Issues, Prevention, and Solutions*. Academic Press. <https://doi.org/10.1016/C2018-0-01939-8>.
- Li, Y., Liu, Z., Jiang, Q., Ye, Y., Zhao, Y., 2022. Effects of nanoplastic on cell apoptosis and ion regulation in the gills of *Macrobrachium nipponense*. *Environ. Pollut.* 300, 118989. <https://doi.org/10.1016/j.envpol.2022.118989>.
- Lin, H.Q., Burden, P.M., Christie, M.J., Johnston, G.A., 1999. The anxiogenic-like and anxiolytic-like effects of MDMA on mice in the elevated plus-maze: a comparison with amphetamine. *Pharmacol. Biochem. Behav.* 62, 403–408. [https://doi.org/10.1016/S0091-3057\(98\)00191-9](https://doi.org/10.1016/S0091-3057(98)00191-9).
- Lins, T.F., O'Brien, A.M., Zargartalebi, M., Sinton, D., 2022. Nanoplastic state and fate in aquatic environments: multiscale modeling. *Environ. Sci. Technol.* 56, 4017–4028. <https://doi.org/10.1021/acs.est.1c03922>.
- Lisney, T.J., Collin, S.P., Kelley, J.L., 2020. The effect of ecological factors on eye morphology in the western rainbowfish, *Melanotaenia australis*. *J. Exp. Biol.* 223. <https://doi.org/10.1242/jeb.223644>.

- Liu, Z., Yu, P., Cai, M., Wu, D., Zhang, M., Huang, Y., et al., 2019. Polystyrene nanoplastic exposure induces immobilization, reproduction, and stress defense in the freshwater cladoceran *Daphnia pulex*. *Chemosphere* 215, 74–81. <https://doi.org/10.1016/j.chemosphere.2018.09.176>.
- Liu, Y., Wang, Y., Ling, X., Yan, Z., Wu, D., Liu, J., et al., 2021a. Effects of nanoplastics and butyl methoxydibenzoylmethane on early zebrafish embryos identified by single-cell RNA sequencing. *Environ. Sci. Technol.* 55, 1885–1896. <https://doi.org/10.1021/acs.est.0c06479>.
- Liu, Z., Li, Y., Pérez, E., Jiang, Q., Chen, Q., Jiao, Y., et al., 2021b. Polystyrene nanoplastic induces oxidative stress, immune defense, and glycometabolism change in *Daphnia pulex*: application of transcriptome profiling in risk assessment of nanoplastics. *J. Hazard. Mater.* 402, 123778. <https://doi.org/10.1016/j.jhazmat.2020.123778>.
- Liu, Z., Li, Y., Sepúlveda, M.S., Jiang, Q., Jiao, Y., Chen, Q., et al., 2021c. Development of an adverse outcome pathway for nanoplastic toxicity in *Daphnia pulex* using proteomics. *Sci. Total Environ.* 144249. <https://doi.org/10.1016/j.scitotenv.2020.144249>.
- Liu, Y., Wang, Y., Li, N., Jiang, S., 2022. Avobenzone and nanoplastics affect the development of zebrafish nervous system and retinal system and inhibit their locomotor behavior. *Sci. Total Environ.* 806, 150681. <https://doi.org/10.1016/j.scitotenv.2021.150681>.
- Manfra, L., Rotini, A., Bergami, E., Grassi, G., Faleri, C., Corsi, I., 2017. Comparative ecotoxicity of polystyrene nanoplastics in natural seawater and reconstituted seawater using the rotifer *Brachionus plicatilis*. *Ecotoxicol. Environ. Saf.* 145, 557–563. <https://doi.org/10.1016/j.ecoenv.2017.07.068>.
- Manuel, P., Almeida, M., Martins, M., Oliveira, M., 2022. Effects of nanoplastics on zebrafish embryo-larval stages: a case study with polystyrene (PS) and polymethylmethacrylate (PMMA) particles. *Environ. Res.* 213, 113584. <https://doi.org/10.1016/j.envres.2022.113584>.
- Martínez, R., Herrero-Nogareda, L., Van Antrop, M., Campos, M.P., Casado, M., Barata, C., et al., 2019. Morphometric signatures of exposure to endocrine disrupting chemicals in zebrafish eleutheroembryos. *Aquat. Toxicol.* 214, 105232. <https://doi.org/10.1016/j.aquatox.2019.105232>.
- Martin-Folgar, R., Torres-Ruiz, M., de Alba, M., Cañas-Portilla, A.I., González, M.C., Morales, M., 2023. Molecular effects of polystyrene nanoplastics toxicity in zebrafish embryos (*Danio rerio*). *Chemosphere* 312, 137077. <https://doi.org/10.1016/j.chemosphere.2022.137077>.
- Materić, D., Holzinger, R., Niemann, H., 2022a. Nanoplastics and ultrafine microplastic in the dutch Wadden Sea – the hidden plastics debris? *Sci. Total Environ.* 846, 157371. <https://doi.org/10.1016/j.scitotenv.2022.157371>.
- Materić, D., Kjør, H.A., Vallenga, P., Tison, J.-L., Röckmann, T., Holzinger, R., 2022b. Nanoplastics measurements in northern and southern polar ice. *Environ. Res.* 208, 112741. <https://doi.org/10.1016/j.envres.2022.112741>.
- Materić, D., Peacock, M., Dean, J., Futter, M., Maximov, T., Moldan, F., et al., 2022c. Presence of nanoplastics in rural and remote surface waters. *Environ. Res. Lett.* 17, 054036. <https://doi.org/10.1088/1748-9326/ac68f7>.
- Matthews, S., Mai, L., Jeong, C.-B., Lee, J.-S., Zeng, E.Y., Xu, E.G., 2021. Key mechanisms of micro- and nanoplastic (MNP) toxicity across taxonomic groups. *Comp. Biochem. Physiol. C: Toxicol. Pharmacol.* 247, 109056. <https://doi.org/10.1016/j.cbpc.2021.109056>.
- Nguyen, L.P., Bradfield, C.A., 2008. The search for endogenous activators of the aryl hydrocarbon receptor. *Chem. Res. Toxicol.* 21, 102–116. <https://doi.org/10.1021/tx7001965>.
- de Oliveira, A.A.S., Brigante, T.A.V., Oliveira, D.P., 2021. Tail coiling assay in zebrafish (*Danio rerio*) embryos: stage of development, promising positive control candidates, and selection of an appropriate organic solvent for screening of developmental neurotoxicity (DNT). *Water* 13, 119. <https://doi.org/10.3390/w13020119>.
- Osborne, O.J., Johnston, B.D., Moger, J., Balousha, M., Lead, J.R., Kudoh, T., et al., 2013. Effects of particle size and coating on nanoscale ag and TiO2 exposure in zebrafish (*Danio rerio*) embryos. *Nanotoxicology* 7, 1315–1324. <https://doi.org/10.3109/17435390.2012.737484>.
- Parenti, C.C., Ghilardi, A., Della Torre, C., Magni, S., Del Giacco, L., Binelli, A., 2019. Evaluation of the infiltration of polystyrene nanobeads in zebrafish embryo tissues after short-term exposure and the related biochemical and behavioural effects. *Environ. Pollut.* 254, 112947. <https://doi.org/10.1016/j.envpol.2019.07.115>.
- Pedersen, A.F., Meyer, D.N., Petriv, A.V., Soto, A.L., Shields, J.N., Akemann, C., et al., 2020. Nanoplastics impact the zebrafish (*Danio rerio*) transcriptome: associated developmental and neurobehavioral consequences. *Environ. Pollut.* 266, 115090. <https://doi.org/10.1016/j.envpol.2020.115090>.
- Peng, L., Fu, D., Qi, H., Lan, C.Q., Yu, H., Ge, C., 2020. Micro- and nano-plastics in marine environment: source, distribution and threats — a review. *Sci. Total Environ.* 698, 134254. <https://doi.org/10.1016/j.scitotenv.2019.134254>.
- Pitt, J.A., Kozal, J.S., Jayasundara, N., Massarsky, A., Trevisan, R., Geitner, N., et al., 2018. Uptake, tissue distribution, and toxicity of polystyrene nanoparticles in developing zebrafish (*Danio rerio*). *Aquat. Toxicol.* 194, 185–194. <https://doi.org/10.1016/j.aquatox.2017.11.017>.
- Poli, E., Angrilli, A., 2015. Greater general startle reflex is associated with greater anxiety levels: a correlational study on 111 young women. *Front. Behav. Neurosci.* 9. <https://doi.org/10.3389/fnbeh.2015.00010>.
- Prut, L., Belzung, C., 2003. The open field as a paradigm to measure the effects of drugs on anxiety-like behaviors: a review. *Eur. J. Pharmacol.* 463, 3–33. [https://doi.org/10.1016/S0014-2999\(03\)01272-X](https://doi.org/10.1016/S0014-2999(03)01272-X).
- Ragusa, A., Svelato, A., Santacroce, C., Catalano, P., Notarstefano, V., Carnevali, O., et al., 2021. Plasticenta: first evidence of microplastics in human placenta. *Environ. Int.* 146, 106274. <https://doi.org/10.1016/j.envint.2020.106274>.
- Repouskou, A., Papadopoulou, A.-K., Panagiotidou, E., Trichas, P., Lindh, C., Bergman, Å., et al., 2020. Long term transcriptional and behavioral effects in mice developmentally exposed to a mixture of endocrine disruptors associated with delayed human neurodevelopment. *Sci. Rep.* 10, 9367. <https://doi.org/10.1038/s41598-020-66379-x>.
- Rey, A.D., Chrousos, G., Besedovsky, H., 2008. *The Hypothalamus-Pituitary-Adrenal Axis*: Elsevier Science. <https://www.elsevier.com/books/the-hypothalamus-pituitary-adrenal-axis/del-rey/978-0-444-53040-0>.
- Rhodes, C.J., 2018. Plastic pollution and potential solutions. *Sci. Prog.* 101, 207–260. <https://doi.org/10.3184/003685018X15294876706211>.
- Roberts, A.C., Reichl, J., Song, M.Y., Dearinger, A.D., Moridzadeh, N., Lu, E.D., et al., 2011. Habituation of the C-start response in larval zebrafish exhibits several distinct phases and sensitivity to NMDA receptor blockade. *PLoS One* 6, e29132. <https://doi.org/10.1371/journal.pone.0029132>.
- Roberts, A.C., Pearce, K.C., Choe, R.C., Alzagatiti, J.B., Yeung, A.K., Bill, B.R., et al., 2016. Long-term habituation of the C-start escape response in zebrafish larvae. *Neurobiol. Learn. Mem.* 134, 360–368. <https://doi.org/10.1016/j.nlm.2016.08.014>.
- Saint-Amant, L., Drapeau, P., 1998. Time course of the development of motor behaviors in the zebrafish embryo. *J. Neurobiol.* 37, 622–632. [https://doi.org/10.1002/\(SICI\)1097-4695\(199812\)37:4<622::AID-NEU10>3.0.CO;2-S](https://doi.org/10.1002/(SICI)1097-4695(199812)37:4<622::AID-NEU10>3.0.CO;2-S).
- Sant, K.E., Timme-Laragy, A.R., 2018. Zebrafish as a model for toxicological perturbation of yolk and nutrition in the early embryo. *Current Environ. Health Reports* 5, 125–133. <https://doi.org/10.1007/s40572-018-0183-2>.
- Schallek, W., Schlosser, W., 1979. Neuropharmacology of sedatives and anxiolytics. *Mod. Probl. Pharmacopsychiatry* 14, 157–173. <https://doi.org/10.1159/000401211>.
- Schnörr, S.J., Steenbergen, P.J., Richardson, M.K., Champagne, D.L., 2012. Measuring thigmotaxis in larval zebrafish. *Behav. Brain Res.* 228, 367–374. <https://doi.org/10.1016/j.bbr.2011.12.016>.
- Schwabl, P., Köppel, S., Königshofer, P., Bucsis, T., Trauner, M., Reiberger, T., et al., 2019. Detection of various microplastics in human stool. *Ann. Intern. Med.* 171, 453–457. <https://doi.org/10.7326/M19-0618>.
- Seralini, G.-E., Jungers, G., 2021. Endocrine disruptors also function as nervous disruptors and can be renamed endocrine and nervous disruptors (ENDs). *Toxicol. Rep.* 8, 1538–1557. <https://doi.org/10.1016/j.toxrep.2021.07.014>.
- Shan, S., Zhang, Y., Zhao, H., Zeng, T., Zhao, X., 2022. Polystyrene nanoplastics penetrate across the blood-brain barrier and induce activation of microglia in the brain of mice. *Chemosphere* 298, 134261. <https://doi.org/10.1016/j.chemosphere.2022.134261>.
- Shankar, P., Dasgupta, S., Hahn, M.E., Tanguay, R.L., 2016. A review of the functional roles of the zebrafish aryl hydrocarbon receptors. *Toxicological Sciences* 178, 215–238. <https://doi.org/10.1093/toxsci/kfaa143>.
- Summers, S., Henry, T., Gutierrez, T., 2018. Agglomeration of nano- and microplastic particles in seawater by autochthonous and de novo-produced sources of exopolymeric substances. *Mar. Pollut. Bull.* 130, 258–267. <https://doi.org/10.1016/j.marpolbul.2018.03.039>.
- Tao, Y., Li, Z., Yang, Y., Jiao, Y., Qu, J., Wang, Y., et al., 2022. Effects of common environmental endocrine-disrupting chemicals on zebrafish behavior. *Water Res.* 208, 117826. <https://doi.org/10.1016/j.watres.2021.117826>.
- Teng, M., Zhao, X., Wu, F., Wang, C., Wang, C., White, J.C., et al., 2022. Charge-specific adverse effects of polystyrene nanoplastics on zebrafish (*Danio rerio*) development and behavior. *Environ. Int.* 163, 107154. <https://doi.org/10.1016/j.envint.2022.107154>.
- Torres-Ruiz, M., De la Vieja, A., de Alba Gonzalez, M., Lopez, M.E., Calvo, A.C., Portilla, A.I.C., 2021. Toxicity of nanoplastics for zebrafish embryos, what we know and where to go next. *Sci. Total Environ.* 149125. <https://doi.org/10.1016/j.scitotenv.2021.149125>.
- Trevisan, R., Voy, C., Chen, S., Di Giulio, R.T., 2019. Nanoplastics decrease the toxicity of a complex PAH mixture but impair mitochondrial energy production in developing zebrafish. *Environ. Sci. Technol.* 53, 8405–8415. <https://doi.org/10.1021/acs.est.9b02003>.
- Trushna, T., Dhiman, V., Raj, D., Tiwari, R.R., 2021. Effects of ambient air pollution on psychological stress and anxiety disorder: a systematic review and meta-analysis of epidemiological evidence. *Rev. Environ. Health* 36, 501–521. <https://doi.org/10.1515/reveh-2020-0125>.
- Ullah, R., Tsui, M.T.-K., Chow, A., Chen, H., Williams, C., Ligaba-Osena, A., 2023. Micro (nano)plastic pollution in terrestrial ecosystem: emphasis on impacts of polystyrene on soil biota, plants, animals, and humans. *Environ. Monit. Assess.* 195, 252. <https://doi.org/10.1007/s10661-022-10769-3>.
- Van Pomeroy, M., Brun, N., Peijnenburg, W., Vijver, M., 2017. Exploring uptake and biodistribution of polystyrene (nano) particles in zebrafish embryos at different developmental stages. *Aquat. Toxicol.* 190, 40–45. <https://doi.org/10.1016/j.aquatox.2017.06.017>.
- Vaz, V.P., Nogueira, D.J., Vicentini, D.S., Matias, W.G., 2021. Can the sonication of polystyrene nanoparticles alter the acute toxicity and swimming behavior results for *Daphnia magna*? *Environ. Sci. Pollut. Res.* 28, 14192–14198. <https://doi.org/10.1007/s11356-021-12455-2>.
- Wahl, A., Le Juge, C., Davranche, M., El Hadri, H., Grassl, B., Reynaud, S., et al., 2021. Nanoplastic occurrence in a soil amended with plastic debris. *Chemosphere* 262, 127784. <https://doi.org/10.1016/j.chemosphere.2020.127784>.
- Walczak, A.P., Kramer, E., Hendriksen, P.J., Tromp, P., Helsper, J.P., van der Zande, M., et al., 2015. Translocation of differently sized and charged polystyrene nanoparticles in *in vitro* intestinal cell models of increasing complexity. *Nanotoxicology* 9, 453–461. <https://doi.org/10.3109/17435390.2014.944599>.
- Walter, K.M., Miller, G.W., Chen, X., Harvey, D.J., Puschner, B., Lein, P.J., 2019. Changes in thyroid hormone activity disrupt photomotor behavior of larval zebrafish. *Neurotoxicology* 74, 47–57. <https://doi.org/10.1016/j.neuro.2019.05.008>.
- Wang, Y., Zhang, Y., Li, X., Sun, M., Wei, Z., Wang, Y., Gao, A., Chen, D., Zhao, X., Feng, X., 2015. Exploring the effects of different types of surfactants on zebrafish embryos and larvae. *Sci. Rep.* 5, 10107. <https://doi.org/10.1038/srep10107>.
- Weber, M., Schmitt, A., Wischmeyer, E., Döring, F., 2008. Excitability of pontine startle processing neurones is regulated by the two-pore-domain K⁺ channel TASK-3 coupled to 5-HT_{2C} receptors. *Eur. J. Neurosci.* 28, 931–940. <https://doi.org/10.1111/j.1460-9568.2008.06400.x>.
- Westphal, N.J., Seasholtz, A.F., 2006. CRH-BP: the regulation and function of a phylogenetically conserved binding protein. *Front. Biosci.* 11, 1878–1891. <https://doi.org/10.2741/1931>.

- Yang, M., Wang, W.-X., 2023. Recognition and movement of polystyrene nanoplastics in fish cells. *Environ. Pollut.* 316, 120627. <https://doi.org/10.1016/j.envpol.2022.120627>.
- Zhang, Y., Goss, G.G., 2020. Potentiation of polycyclic aromatic hydrocarbon uptake in zebrafish embryos by nanoplastics. *Environ. Sci. Nano* 7, 1730–1741. <https://doi.org/10.1039/D0EN00163E>.
- Zhang, R., Silic, M.R., Schaber, A., Wasel, O., Freeman, J.L., Sepulveda, M.S., 2020a. Exposure route affects the distribution and toxicity of polystyrene nanoplastics in zebrafish. *Sci. Total Environ.* 724, 138065. <https://doi.org/10.1016/j.scitotenv.2020.138065>.
- Zhang, Y., Kang, S., Allen, S., Allen, D., Gao, T., Sillanpää, M., 2020b. Atmospheric microplastics: a review on current status and perspectives. *Earth Sci. Rev.* 203, 103118. <https://doi.org/10.1016/j.earscirev.2020.103118>.
- Zhang, Y., Zhang, X., Yan, Q., Xu, C., Liu, Q., Shen, Y., et al., 2022. Melatonin attenuates polystyrene microplastics induced motor neurodevelopmental defect in zebrafish (*Danio rerio*) by activating nrf2 - isl2a Axis. *Ecotoxicol. Environ. Saf.* 241, 113754. <https://doi.org/10.1016/j.ecoenv.2022.113754>.
- Zhao, H.J., Xu, J.K., Yan, Z.H., Ren, H.Q., Zhang, Y., 2020. Microplastics enhance the developmental toxicity of synthetic phenolic antioxidants by disturbing the thyroid function and metabolism in developing zebrafish. *Environ. Int.* 140, 105750. <https://doi.org/10.1016/j.envint.2020.105750>.